New drug targets and therapeutic approaches in heart failure

PhD thesis

Author: Adam Riba

Program leader: Professor Kalman Toth, MD, DSc

Project leader: Eszter Szabados MD, PhD

Robert Halmosi MD, PhD

First Department of Medicine

University of Pécs School of Medicine

Hungary

2017

Contents

1 Abbrevations

ACE-I: angiotensin converting enzyme inhibitor

Akt-1: RAC-alpha serine/threonine-protein kinase

AMPK: AMP-activated protein kinase

ARB: aldosteron receptor blocking drug

BNP: B-type natriuretic peptide

BW: body weight

CAD: coronary artery disease

COX: cyclooxygenase

CHF: Chronic Heart Failure

DOX: doxycycline

Drp-1: dynamin-related protein 1

EF: ejection fraction

ERK 1/2: extracellular signal-regulated kinase 1/2

ESC: European Society of Cardiology

ETC: electron transport chain

FS: fractional shortening

GAPDH: Glycerolaldehyde-3-phosphate dehydrogenase

GSK-3β: glycogen synthase kinase-3β

HF: heart failure

HFpEF: HF with preserved EF

HFrEF: HF with reduced EF

HFmrEF: heart failure with mid-range ejection fraction

iNOS: inducible nitric oxide synthase

I/R: ischemia-reperfusion

ISO: isoproterenol hydrochloride

IVS (d): thickness of interventricular septum in diastole

IVS (s): thickness of interventricular septum in systole

JC-1: cationic carbocyanine dye

LAD: left anterior descending

LC-3: Microtubule-associated protein 1A/1B-light chain 3

LV: left ventricle

LVEDV: left ventricular end-diastolic volume

LVESV: left ventricular end-systolic volume

LVID (d): left ventricular end-diastolic diameter

LVID (-s): left ventricular end-systolic diameter

MAPK: mitogen-activated protein kinase

Mfn-2: mitofusin-2

MI: myocrdial infarction

MKP-1: mitogen-activated protein (MAP) kinase-phophatase-1

MTT: 3-[4,5-dimethylthiazol-2-yl]-2,5-diphenyltetrazolium bromide

NF-KB: nuclear factor kappa B

NIH: National Institute of Health

NT: nitrotyrosine

OPA-1: mitochondrial dynamin-related GTPase

PAR: poly(ADP-ribose) polymer

PARP: poly(ADP-ribose) polymerase

PKC: protein kinase c

PO: pressure overload

PW (d): thickness of left ventricular posterior wall in diastole

PW (s): thickness of left ventricular posterior wall in systole

RAAS: renin-angiotensin-aldosterone system

RES: resveratrol (3,5,4'-trihydroxystilbene)

ROS: reactive oxygen species

RyR: ryanodine receptor

RWT: relative wall thickness

SEM: standard error of mean

SIRT1: sirtuin 1

TAC: transverse aortic constriction

TBS: TRIS-buffered saline

TL: tibia length

VW: ventricular weight

VO: volume overload

WKY: Wistar-Kyoto Rat

2 Introduction

2.1 Definition and forms of heart failure

The 2016 European Society of Cardiology Guidelines for the diagnosis and treatment of acut and chronic heart failure defines heart failure as a „clinical syndrome characterized by typical symptoms (e.g. breathlessness, ankle swelling and fatigue) that may be accompanied by signs (e.g. elevated jugular venous pressure, pulmonary crackles and peripheral oedema) caused by a structural and/or functional cardiac abnormality, resulting in a reduced cardiac output and/or elevated intracardiac pressures at rest or during stress." (1)

Heart failure (HF) is often, but not always, resulted from a myocardial dysfunction, caused by myocardial ischemia, myocarditis or primer myocardial diseases. In other cases a sudden load exceeds the capacity of the heart (e.g. acute aortic regurgitation, tachyarrhytmias) or the ventricular filling is impaired (e.g. mitral stenosis, constrictive pericarditis). Before clinical symptoms become apparent, it is important to recognize the causes and precipitating factors of HF and start treating them to prevent poor outcomes (2).

Focusing on hemodynamics we can talk about *forward versus backward HF*. In forward HF the clinical symptoms are mainly due to the inadequate delivery of blood into the arterial system causing organ failure, most tipically renal failure. In backward HF the ventricle fails to empty its contents, blood accumulates and pressure rises in the atrium and venous system increasing the fluid in lungs, liver, subcutan tissues and serous cavities. Depending on the initially affected cardiac chamber we may define *left-sided versus right-sided HF*. We may also distinguish *acut versus chronic HF* depending on the rate at which syndrome develops. *Low-output HF* refers to the marked reduction in the stroke volume causing systemic vasoconstriction while *high-output HF* may develop in thyrotoxicosis and anemia. We can also define s*ystolic versus diastolic HF*. In systolic HF mainly the systole, in diastolic HF principally the ventricular filling (diastole) is affected (2).

There are two major types of HF based on the measurement of the left ventricular ejection fraction (LVEF): 1. Patients with normal LVEF (typically considered as ≥50%), referred to as HF with preserved EF (HFpEF). 2. Patients with reduced LVEF (typically considered as below 40%), referred to as HF with reduced EF (HFrEF). Patients with an LVEF in the range of 40–49% represent a 'grey area', which we now define as heart failure with mid-range ejection fraction (HFmrEF). In my present work I mainly focus on HFrEF (3).

2.2 Epidemiology of heart failure

Despite advances in pharmacological and interventional cardiology heart failure remains a leading cause of morbidity and mortality in Europe or North America. The prevalence of HF depends on the definition applied, but is approximately 2% of the adult population in developed countries, rising to ≥10% among people >70 years of age (4). From the 1970s to 1990s, a dramatic increase in the prevalence of HF and number of HF hospitalizations was observed, and an epidemic was declared. Most of the HF burden is borne by individuals aged ≥65 years, who account for more than 80% of the deaths and prevalent cases in the USA and Europe. The growing prevalence of HF might reflect increasing incidence, an aging population, improvements in the treatment of acute cardiovascular disease and HF or a combination of these factors (5).

2.3 Pathophysiology of heart failure

Heart failure can be caused by a wide number of conditions, including coronary artery disease (myocardial infarction or chronic hypoperfusion), long-term hypertension, valvular and pericardial diseases, toxic agents (alcohol or drugs), cardiac infections and inflammation, long term arrythmias, congenital diseases (cardiomyopathies), and high-output states (anemia, thyreotoxicosis). A reduced stroke volume may occur as a result of a failure of systole, diastole or both.

When heart failure develops several adaptive mechanisms are activated to maintain normal circulation. Most important among these are 1. the Frank-Starling mechanism in which an increased preload helps to maintain cardiac performance; 2. activation of the renin-angiotensin-aldoszteron system (RAAS), the sympathetic nervous system and other neurohumoral factors (natriuretic peptides, vasopressin, endothelin etc.) aimed to increase cardiac contractility and maintain arterial pressure and perfusion of vital organs; 3. myocardial remodeling in which the mass of contractile tissue is augmented. The first two of these adaptive mechanisms developes rapidly, while myocardial remodeling and hypertrophy develops slowly and play an important role in long term adaptation. However the prolonged or severe activation of these processes leads to maladaptive changes in the myocardium causing progressive hypertrophy, increased myocardial stiffness due to increased collagen accumulation and eventually dilatation. Along with these macroscopic changes several pathological processes are activated at a cellular level including fetal gene expression, altered calcium handling, adenosine triphosphate (ATP) depletion, energy starvation, activation of different signal transduction pathways, reactive

oxygen species (ROS) overproduction etc. resulting in myocyte death due to apoptosis or necrosis (6).

2.3.1 Oxidative stress in heart failure and role of mitochondria

There are increasing evidence suggesting that ROS play major pathological role in the development and progression of heart failure (7).

ROS can damage cardiac tissue through oxidation of lipids, proteins and DNA, producing diverse effects such as reduced cardiac contractility, malfunction of ion transporters, and calcium cycling (8). Their toxic effects are limited by free radical scavengers such as superoxide dismutase (SOD) which catalyzes the formation of hydrogen-peroxide (H_2O_2) from superoxide ($O_2^{-\cdot}$), glutathione peroxidase, catalase which catalyzes the breakdown of H_2O_2 to water, and other non-enzymatic antioxidants such as vitamins E, C and β-carotene, ubiquinone (coenzyme Q10), lipoic acid and urate (9). There is no deficiency of these enzymatic defenses in heart failure, although manganese SOD protein may be reduced; hence damage may ensue from excessive production of ROS. In addition, ROS can also act as an intracellular signaling mechanism, affecting transcription factors such as NF-KB and activator protein-1. The chronic exposure to ROS leads to further deterioration of heart muscle resulting in cardiac remodeling, apoptosis, necrosis, and fibrosis (10).

Mitochondria are primarily responsible for ATP synthesis but under pathophysiological conditions, they become the main sources of endogenous ROS production (11). Side reactions of oxygen with mitochondrial respiratory enzymes (primarily complex I and III) directly generate superoxide anion radical. The superoxide radicals can react with nitric oxide (NO) to form peroxynitrite, a highly reactive and deleterious free radical species, or can be converted by SOD to H_2O_2 that can further react to form highly reactive hydroxyl radicals. Mitochondrial-generated ROS can lead to extensive oxidative damage to proteins, DNA, and lipids, particularly targeting proximal mitochondrial components including mitochondrial respiratory enzymes, matrix enzymes (e.g., aconitase), and membrane phospholipids, such as cardiolipin.

Mitochondria are dynamic intracellular organelles, and they change their morphology by undergoing either fusion or fission, resulting in either elongated, tubular, interconnected mitochondrial networks or fragmented, discontinuous mitochondria, respectively.

A balance in mitochondrial fusion and fission is essential in the maintenance of mitochondrial networks and critical for cardiac metabolism and heart function (12). Oxidative conditions deteriorate this subtle balance (13). Mitochondrial fusion and fission are regulated by dynamin-like guanosine triphosphatases (GTPases) such as mitofusin 2 (Mfn-2), optic atrophy 1 (OPA-

1) and dynamin-related protein 1 Drp-1 (14, 15), which are markedly induced by oxidative stress (16). Regarding Mfn-1 and Mfn-2 they both produce connected mitochondria and make large mitochondrial networks (13). However, only Mfn-2 connects mitochondria to the endoplasmatic reticuli. This connection between ER and mitochondria results in Ca2+ influx into the mitochondria, leading to fragmentation (17, 18) (Fig. 1).

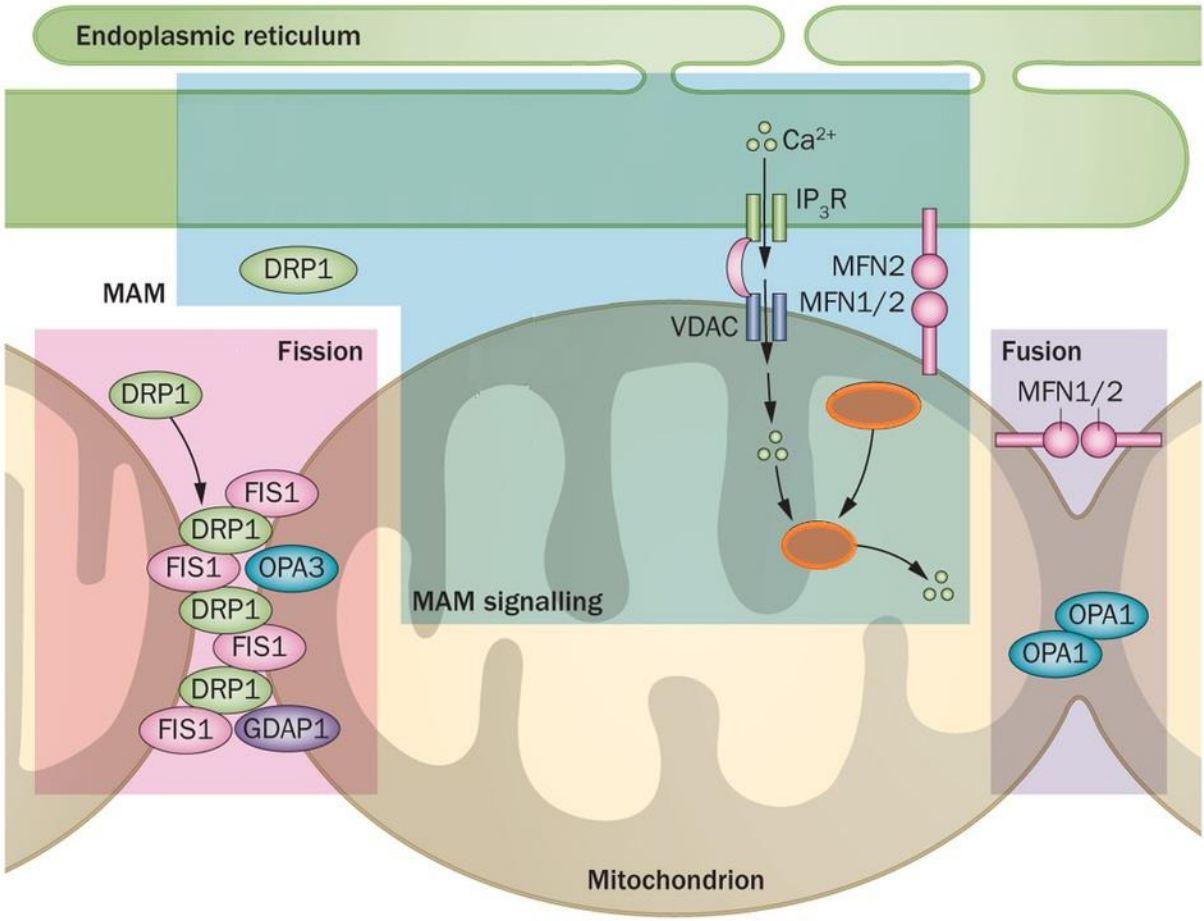

Fig 1: Mitochondrial dynamics and interactions: Mitochondria-associated ER membranes (MAM) is a mechanism which results from communication between endoplasmic reticulum (ER) and mitochondria, this linkage consist of some proteins and a region on ER containing lipid biosynthetic enzyme connected reversibly to mitochondria. Mitochondria associated membranes are involved in the transport of calcium from the ER to mitochondria. This interaction is important for rapid uptake of calcium by mitochondria through Voltage dependent anion channels (VDACs), which are located at the outer mitochondrial membrane (OMM) mitofusin 2 (Mfn-2), optic atrophy 1 (OPA-1) and dynamin-related protein 1 Drp-1. OPA-1, Mfn-1 and Mfn-2 are essential mediators of the sequential fusion of the outer and inner membranes of adjacent mitochondria. During fission, DRP1 is recruited from the cytosol to the outer mitochondrial membrane. This figure was inserted from the article

of Florence Burté et al. Disturbed mitchondrial dynamics and neurodegenrative disorders (Nature Rewievs Neurology 11, 11-24 (2015))

According to the literature inhibition of Mfn-2 leads to large mitochondrial networks without connecting the mitochondria to the ER, preventing fragmentation. Mfn-1 and Mfn-2 both induce outer mitochondrial membrane fusion and fission, whereas OPA-1 is required for inner mitochondrial membrane fusion and it was observed that uncleaved, fusion active OPA-1 is sufficient to maintain cardiac activity (19). Fragmentation is also executed by Drp-1, a cytosolic protein that is recruited to the mitochondrial surface by phosphorylation in response to oxidative stress. A fragmentation of the mitochondrial network occurs in response to cellular stress and is observed in a wide variety of disease conditions, including heart failure via the modulation of ion transporters and calcium cycling (20-22).

2.3.2 The role of intracellular signaling pathways in the pathophysiology of heart failure

Pathological remodeling of the heart is accompanied by alterations in cardiac gene expression resulting in the shift from the activation of prosurvival factors (RAC-alpha serine/threonine-protein kinase - Akt-1, glycogen synthase kinase-3β – GSK-3β) towards the activation of disadvantageous signaling factors (p38-mitogen activated protein kinase - p38-MAPK, inducible nitrogen oxide synthase - iNOS, cyclooxigenase-2 - COX-2, nuclear factor- κB - NF-κB) (23).

NF-κB, COX-2 and iNOS promotes adverse remodeling, apoptosis and the downregulation of cardiomyocyte contractility. Previous studies showed that COX-2 is upregulated by p38-MAPK and extracellular signal-regulated kinase 1/2 (ERK1/2) (24). Moreover, prolonged activation of COX-2 produces cardiac cell death, leading to gradual loss of myocardial function and eventually heart failure. The inducible nitric oxide synthase (iNOS) generates a prolonged release of large amounts of nitrogen-oxide (NO) which may be cytotoxic and/or inhibit myocyte contractility (25, 26).

Large number of physiological, pharmacological and pathological stimuli initiate cardiac hypertrophy. In addition, cardiac hypertrophy is associated with alterations in intracellular signal transduction pathways, including alterations of G-protein-coupled receptor signaling, mitogen activated protein kinase (MAPK), protein kinase C (PKC), calcineurin and calmodulin. Various signaling pathways are involved in the complicated interactions that finally promote cardiac hypertrophy and HF (27, 28).

There are increasing numbers of evidence suggesting that normal cardiac growth and exercise-induced hypertrophy are mainly regulated by the phosphatidil-inositol-3 kinase (PI3K)/Akt pathway. Akt has multiple downstream targets: one of them is GSK-3β. Recent studies revealed an important role for Akt-signaling in cardiac angiogenesis and in blocking the transition from hypertrophy to HF (29).

Growing data suggest that aiming the modulation of MAPK cascades could be a promising target to treat cardiomyocyte hypertrophy and HF. The MAPKs are elements of three-tiered protein kinase cascades and comprise basically three subfamilies, the ERKs, c-jun N-terminal kinases (JNKs) and the p38-MAPKs. The exact role of MAPKs is still controversial in chronic heart failure (CHF). It was reported that ERK 1/2 activation leads to a concentric form of hypertrophy with enhanced cardiac function (19) and dual specificity mitogen-activated protein kinase kinase 1/2 (MEK1/2) protects the heart from ischemia induced apoptotic insults in mice (23).

2.4 Current pharmacological treatment strategies in chronic heart failure

Heart failure (HF) is a major health problem in the western world, in spite of the development in its treatment over the last 30 years. The greatest advance has been the application of agents that inhibit harmful neurohormonal activation in the treatment of HF. Inhibiton of the RAAS with angiotensin converting enzyme inhibitors (ACE-I) or angiotensin receptor blockers (ARB) if ACE-Is are contraindicated or not tolerated, and inhibition of the sympathetic nervous system with beta-adrenergic blocking agents are first-line threrapy for people with chronic heart failure (1).

Mineralocorticoid/aldosterone receptor antagonists (spironolactone, eplerenone) have also shown to reduce both morbidity and mortality of HFrEF patients in large clinical trials. Therefore current guidelines from the American Heart Association and ESC recommend their use in all symptomatic HFrEF patients with LVEF ≤35%, to reduce mortality and HF hospitalization (30, 31).

Ivabradine should also be considered to reduce symptoms and hospitalization in symptomatic patients with LVEF ≤35%, in sinus rhythm and a resting heart rate ≥70 bpm despite treatment with an evidence-based dose of beta blocker (or maximal tolerated dose), ACE-I (or ARB), and an mineralocorticoid receptor antagonists (MRA) (30, 31).

With the exception of the aldosterone antagonists, diuretics do not influence the natural history of HF. However diuretics improve congestive sympoms and may also slow the progression of

ventricular remodeling by reducing ventricular filling pressure and wall stress. It should also be emphasized that the overdose of diuretics increase the activity of the adrenergic system.
Digoxin, long-acting nitrate, vasodilators can also be used to reduce symptoms and hospitalizations (1, 30).

2.5 New therapeutic approaches in the treatment of HF

For years, therapeutic approaches for heart failure (HF) relied on vasodilators and diuretics which relieve cardiac workload and HF symptoms. The introduction of antiadrenergic agents and the inhibitors of the renin-angiotensin-aldosterone system has substantially ameliorated survival. The current therapy, though, is still unable to restore muscle function fully, and the development of novel therapeutic targets are essential in the future therapy of HF. Understanding the molecular basis of myocardial dysfunction and remodeling may help researchers for developing new treatments capable of restoring muscle function or slow the progression of HF. In A position paper from the Working Group on Myocardial Function of the ESC titled „Targeting myocardial remodeling to develop novel therapies for heart failure" discusses novel molecular targets with potential therapeutic impact including omecamtiv mecarbil (a myosin activator), nitroxyl (HNO) donors (like CXL-1020 improving myocyte function), cyclosporin A (inhibiting mitochondrial permeability transition pore opening and cell death), SERCA2a (sarcoplasmic/endoplasmic Ca^{2+} ATPase 2a, improving Ca^{2+} uptake in the sarcoplasmic reticulum), neuregulin1 (enhancing protective signaling), VEGF-A, VEGF-B (regulating cardiac angiogenesis) and others (32).
Our working group has also several promising preclinical results with different PARP inhibitors on cardiac hypertrophy (23), remodeling (29) and vascular damage of hypertension (33).
Furthermore many studies have previously examined drugs targeting mitochondrial energy metabolism and ROS production, but most of them have failed to alleviate cardiac damage in clinical investigations, demonstrating the complexity of the processes occurring in the mitochondria (8).

2.6 Cardiac effects of a well-known antibiotic: doxycycline

Doxycycline (Dox) is a well-known antibiotic agent with a minimal amount of side-effects. It is used in the treatment of many bacterial infections, such as acne, urinary, gastrointestinal or eye infections, gonorrhea, chlamydia and Lyme's disease. Besides DOX has a well established matrix metalloproteinase (MMP) (MMP-2 and 9) (34, 35) inhibitory effect, which is believed to be the

base of its major protective effect in the acute phase of myocardial infarction and in the early phase of myocardial remodeling (36, 37) (38). Matrix metalloproteinases (MMPs) are a family of proteolytic enzymes responsible for myocardial extracellular protein degradation. Several MMP species may be dysregulated in congestive heart failure leading to left ventricular (LV) remodeling. Tissue inhibitors of the MMPs (TIMPs) are locally synthesized proteins that bind to active MMPs and thereby regulate net proteolytic activity. However, there is no concomitant increase in myocardial TIMPs during the LV remodeling, and a persistent MMP activation state within the myocardium likely contributes to the LV remodeling process (39). Doxycycline is a potent inhibitor of MMPs and exhibits MMPs inhibition in vivo at blood levels lower than those required for its antibacterial effect (40). It effectively crosses cell membranes, accumulates preferentially in cardiomyocytes (41), and inhibits mainly the MMP-9 and -2,(42) which are largely up-regulated in the setting of animal(43) and human(44) remodelled hearts after MI. Accordingly, pre-clinical studies showed that timed treatment with doxycycline significantly attenuates post-infarct LV remodeling (45). Moreover, doxycycline has showed a cardioprotective effect in isolated animal hearts subjected to ischaemia/reperfusion injury (46, 47). Given the clinical availability and well-recognized safety profile of Dox it has been used in one clinical trial in patients with acute ST-elevation myocardial infarction with LV dysfunction, where DOX reduced myocardial infarct size and adverse LV remodeling (48).

2.7 Resveratrol, a natural polyphenolic compound with numerous beneficial cardiac effects

Phenolic compounds are chemically classified into flavonoids and non-flavonoids. Flavonoids include flavonols (quercetin, kaempferol, etc.), flavones (apigenin, luteolin, etc.), flavan-3-ols (catechin, epicatechin, etc.), proanthocyanidins (procyanidins B1, B2, etc.), flavanones (hesperidin, etc.), anthocyanins (malvidin, cyanidin, etc.) and isoflavones (genistein, etc.). Non-flavonoids (49) include hydroxycinnamic acids (chlorogenic acid, caffeic acid, etc.), hydrolyzable tannins such as ellagitannins (punicalagin, etc.) and gallotannins (pentagalloyl glucose, etc.), hydroxybenzoic acids (gallic acid, etc.) and stilbenes (resveratrol, piceid, viniferins, etc (50). Resveratrol (3,5,4'-trihydroxystilbene) (RES) - Figure (Fig) 7 - is primarily found in grapes, red wine, nuts and some type of berries (51). Numerous experimental studies have verified that RES interferes with several pathological processes in different cardiovascular diseases such as myocardial ischemia (52), myocarditis (53), cardiac hypertrophy (54) and heart failure (55). Multiple mechanisms have been proposed to be responsible for the protective effect of resveratrol, including reducing oxidative stress and inflammation (56, 57), inhibition of pathological hypertrophic signaling and Ca2+ handling (55, 58), affecting different intracellular

signaling pathways, such as sirtuin 1 (SIRT1) (59), AMP-activated protein kinase (AMPK), mitochondrial function, fibrosis etc (60). The vast majority of these studies are in vitro or animal studies, and only a few clinical studies can be found (50). Previously our working group examined RES in a clinical study in patients with established coronary artery disease (CAD) and verified that RES improved left ventricle diastolic function (no efffect on systolic function was observed), endothelial function, lowered LDL-cholesterol level and protected against unfavourable hemorheological changes after 3 months of oral administration of 10 mg RES (61).

In my present work I will mainly focus on the effect of RES in heart failure in an animal model. Sung et al summarized all animal studies available in the literature regarding the cardiac effects, doses, duration and possible molecular mechanism of RES treatment in different heart failure models including myocardial infarction, pressure overload, hypertensive, myocarditis or chemotherapy induced and genetic models of HF (Table 1). As we can see in Table 1 different -molecular mechanisms are involved in RES treatment but the most frequently mentioned protective effect was its antioxidant property.

Table 1. Resveratrol in animal models of heart failure

Animal model	Resveratrol dose	Duration	Effect	Potential molecular mediators
Myocardial infarction				
Rats with LAD ligation induced MI	5 mg/kg/day starting 1-week before MI—orally	4 weeks	Reduced ventricular tachycardia and fibrillation and reduced infarct size, hypertrophy, and mortality	Resv inhibited L-type calcium channels and selectively enhanced ATP-sensitive K+ channels
Rats with LAD ligation induced MI	0.1 or 1.0 mg/kg/day i.p. starting 6 hours postsurgery	4 weeks	No effect of 0.1 mg/kg/day on cardiac function. 1.0 mg/kg/day improved cardiac function and reduced infarct size	Resv reduced expression of ANP and TGFb1 mRNA
Rats with LAD ligation induced MI	2.5 mg/kg/day in the diet starting 1-week postsurgery	16 weeks	Improved cardiac function and survival rate	Increased SIRT1 and AMPK levels
Mice with LAD ligation induced MI*a*	5 or 50 mg/kg/day by s.c. minipump at 4 weeks postsurgery	2 weeks	No effect of 5 mg/kg/day on cardiac function. 50 mg/kg/day improved cardiac function and reduced remodeling and infarct size	Increased SIRT1 and AMPK levels and autophagy

Pressure overload				
Rats with aortic banding to induce PO	2.5 mg/kg/day by oral gavage starting 2 weeks postsurgery	2 weeks	Reduced cardiac hypertrophy and improved diastolic function	Increased eNOS and iNOS levels
Mice with TAC to induce PO	10 mg/kg/day by oral gavage starting 24 hours postsurgery	28 days	Reduced cardiac hypertrophy and remodeling and increased cardiac function	Reduced cardiac fibrosis, inflammation, oxidative stress, and cardiomyocyte apoptosis
Rats with aortic banding to induce PO	2.5 mg/kg/day by oral gavage starting at 2 or 14 days postsurgery	26 or 14 days	Reduced cardiac hypertrophy and improved diastolic function when administered as a preventive and treatment strategy	Reduced oxidative stress
Rats with aortocaval shunt to induce VO	2.5 mg/kg/day by oral gavage starting at 2 days or 14 days postsurgery	26 or 14 days	No effect on cardiac hypertrophy or function	N/A
Rats with abdominal aortic banding	4 mg/kg/day starting at 4 weeks postsurgery	4, 6 or 8 weeks	Prevented cardiac hypertrophy, ventricular dilatation, fibrosis, and systolic dysfunction	Increased SERCA2a and RyR levels and SERCA activity
Mice with TAC to induce PO*a*	320 mg/kg/day in the diet starting 3 weeks postsurgery	2 weeks	Improved diastolic function, cardiac remodeling, and survival	Increased AMPK, insulin sensitivity, and cardiac glucose metabolism
Hypertension				
Spontaneously hypertensive rat (SHR)	2.5 mg/kg/day by oral gavage starting at 10 weeks of age	10 weeks	Prevented the development of cardiac hypertrophy and systolic dysfunction without a change in BP	Reduced oxidative stress
Dahl salt-sensitive rat	18 mg/kg/day in the diet starting at 3 weeks of high salt (8% NaCl)	8 weeks	Preserved cardiac function and survival without a change in BP or hypertrophy	Increased mitochondrial content and ATP production
Myocarditiis				
Rats immunized with cardiac myosin	50 mg/kg/day i.p. starting 1 day before or 1 day after immunization	14 or 21 days	Both treatment protocols reduced cardiac hypertrophy and improved cardiac function	Reduced inflammation and fibrosis
Genetic models of heart failure				

TO-2 hamsters	Diet supplemented with 4 g resveratrol/kg starting at 6 weeks of age	6 or 29 weeks	Improved cardiac function and reduced cardiac hypertrophy and mortality	Reduced oxidative stress and cell death by upregulating antioxidants via SIRT1-dependent pathway
Chemotherapy				
Doxorubicin to induce HF	10 mg/kg/day i.p. for 2 weeks pretreatment, during 2 weeks of Dox and 3 weeks after the last Dox dose	7 weeks	Prevented the development of cardiac dysfunction, cardiac fibrosis, and ventricular dilatation	Reduced oxidative stress
Doxorubicin to induce HF	_320 mg/kg/day in the diet starting at time of first Dox i.p. dose	8 weeks	Prevented the development of cardiac dysfunction, cardiac hypertrophy, and ventricular dilatation and improved exercise capacity	Reduced oxidative stress and increased mitochondrial ETC complexes

This table was inserted from the article of Sung & Dyck et al: Resveratrol in heart failure. [a]Denotes studies where resveratrol was administered as a treatment. Dox, doxorubicin; ETC, electron transport chain; HF, heart failure; i.p., intraperitoneal; LAD, left anterior descending; MI, myocardial infarction; PO, pressure overload; Resv, resveratrol; RyR, ryanodine receptor; s.c., subcutaneous; TAC, transverse aortic constriction; VO, volume overload.

3 Aims of the present work

The aim of our work was to further evaluate the effects of two different compounds in heart failure: doxycycline and resveratrol.

3.1. To further clarify the cardioprotective effect of doxycycline in HF we examined its effect on

a. ROS production and mitochondrial dynamics and fragmentation,
b. cardiac fibrosis,
c. severity of HF featured by BNP, LVEF, gravimetric parameters.

3.2. To further examine the cardioprotective effect of resveratrol in HF, the following experiments were carried out:

a. measurements of echocardiographic parameters with high-resolution imaging system
b. assessing interstitial fibrosis and oxidative stress on histological samples
c. evaluating the steady state phosphorylation and expression levels of intracellular signaling factors: Akt-1, GSK-3B, p38-MAPK, ERK 1/2, MKP-1, COX-2 and iNOS.

4 Examination of doxycycline in a postinfarction heart failure model

4.1 Methods

4.1.1 Cell viability assay

H9c2 rat heart myoblast cells were obtained from the European Collection of Cell Cultures (ECACC) and maintained in Dulbecco's modified Eagle's medium (DMEM) supplemented with 10 % fetal bovine serum (FBS, Invitrogen, Carlsbad, CA, USA), 4 mM glutamine, 100 IU/ml penicillin and 100 ug/ml streptomycin. The effect of H_2O_2 and doxycycline on H9c2 cardiomyocytes was investigated using the Sulforhodamine B (SRB) assay, performed according to the method of Papazisis and colleagues (62), with modifications. H9c2 cells were cultured in 96-well microtiter plates in a humidified 95% O_2/5% CO_2 atmosphere at 37°C. Cells were treated for 2 hours with different concentrations of H_2O_2 (0.2 mM, 0.3 mM, 0.4 mM, 0.5 mM). Fifty percent of cell degradation was detected at the concentration of 0.3 mM H_2O_2. Increasing concentrations of doxycycline (50 nM, 100 nM, 300 nM, 1 μM, 10 μM) were applied to the cells in the subsequent study. Culture medium was aspirated prior to fixation of the cells by addition of 200 μl cold 10% trichloroacetic acid. After a 20 min incubation at 4°C, cells were washed 5 times with deionized water. Microplates were then left to dry at room temperature for at least 24 h. The cells were then stained with 200 μl 0.1% SRB dissolved in 1% acetic acid for at least 20 min at room temperature and subsequently washed 4 times with 1% acetic acid to remove unbound stain. The plates were left to dry at room temperature. Bound SRB was solubilized with 200 μl 10 mM unbuffered Tris-base solution and plates were left on a plate shaker for at least 10 min. Absorbance was read with a GloMax Multi Detection System (Promega, USA) at 560 nm subtracting the background measurement at 620 nm. The test optical density (OD) value was defined as the absorbance of each individual well, minus the blank value ('blank' is the mean optical density of the background control wells). All experiments were performed in triplicate.

4.1.2 Detection of mitochondrial fragmentation with fluorescent microscopy

The H9c2 rat heart myoblast cell line was obtained from the European Collection of Cell Cultures (Salisbury, UK). The cell line was maintained in a humidified 5% CO_2 atmosphere at

37°C. H9c2 cells were cultured in Dulbecco's modified Eagle's medium (PAA Laboratories, Cölbe, Germany) containing 10% bovine serum and antibiotic solution (1% penicillin and streptomycin mixture; Gibco/Invitrogen, Carlsbad, CA). Cells were passaged at 3 day intervals. H9c2 cells were seeded at a starting density of $1x10^5$ cells/well in 6 well plates on glass coverslips and cultured at least overnight before the experiment. The next day, cells were washed twice in PBS, and then treated with H_2O_2 with or without doxycycline. Group of cells: Control: cells without any treatment; DOX: 5 μM doxycycline for 5 hours; H_2O_2: 400 μM H_2O_2 for 5 hours; H_2O_2+DOX: 400 μM H_2O_2 and 5 μM doxycycline for 5 hours. After subjecting cells to the appropriate treatment, coverslips were rinsed twice in modified Krebs-Henseleit solution. To visualize the mitochondria, 50 nM of MitoTracker Red (Molecular Probes) was added and incubated for 15 minutes. The cells were then washed twice in modified Krebs-Henseleit solution and placed upside down on the top of a small chamber formed by a microscope slide and a press-to-seal silicone isolator. The chamber was filled with modified Krebs-Henseleit solution containing 4.5 g/L glucose. The cells were visualized using a Nikon Eclipse Ti-U fluorescent microscope equipped with a Spot RT3 camera using a 60x objective and epifluorescent illumination. Representative merged images of three independent experiments are presented.

4.1.3 Mitochondrial membrane potential measurement with JC-1 assay for fluorescent microscopy

The mitochondrial membrane potential (ΔΨm) was measured using the mitochondrial membrane potential–specific fluorescent probe, JC-1 (Molecular Probes). H9c2 cells were seeded on glass coverslips and cultured at least overnight before the experiment. After treatment, cells were washed twice in ice-cold PBS and then incubated for 5 min at 37°C in modified Krebs-Henseleit solution (118mM NaCl, 5mM KCl, 1.2 mM KH_2PO_4, 25 mM $NaHCO_3$, 5mM glucose, 1.2 mM $MgSO_4x7H_2O$) containing 0.1 μM JC-1. When excited at 488 nm, the dye emits green fluorescence (530 nm) at low ΔΨm and red (590 nm) at high ΔΨm. Following incubation, the cells were washed once with Krebs-Henseleit solution and then imaged with a Nikon Eclipse Ti-U fluorescent microscope equipped with a Spot RT3 camera using a 60x objective and epifluorescent illumination. All experiments were repeated in triplicate.

4.1.4 Animals

Male 16 week old Wistar rats (410–480 g) were used for the experiments. Animals received care according to the Guide for the Care and Use of Laboratory Animals published by the US National Institute of Health (NIH Publication No. 85-23, revised 1996) and the experiment was approved by the Animal Research Review Committee of the University of Pecs, Medical School (Permit number: BA02/2000-2/2010). The animals were housed under standardized conditions, 12 h dark–light cycle in solid bottomed polypropylene cages, and received commercial rat chew *ad libitum*. Doxycycline or tap water was administered as drink *ad libitum* for 8 weeks. We set the dosage of doxycycline to 5 mg/b.w.(kg)/day (29, 36).

4.1.5 Isoproterenol heart failure model

We used the ISO-induced myocardial infarct model that is a relevant murine model of postinfarction heart failure. Subcutaneous administration of isoproterenol produces patchy myocardial necrosis predominantly subendocardially. The significant myocardial cell loss is followed by consequent left ventricular hypertrophy and cardiac fibrosis, the left ventricular function decreases and myocardial remodeling occurs. Eventually these processes are leading to heart failure similar to the one obeserved in post-MI patients. Because isoproterenol is rapidly metabolized, acute adverse effects of the drug can be avoided.

4.1.6 Experimental protocol

To induce postinfarction myocardial remodeling, the rats were treated twice on two consecutive days with 80 mg/kg ISO (Sigma-Aldrich) or vehicle subcutaneously as previously described (63). The animals were divided into the following four groups and were followed for 8 weeks: control group (C, n = 5), received clear tap water without any treatment; ISO group (ISO, n = 7) received two subcutaneous injections of ISO at a dosage of 80 mg/b.w.(kg) and clear tap water afterwards; ISO+doxycycline group (ISO+DOX, n = 7), received 5 mg/b.w.(kg)/day doxycycline after ISO treatment; doxycycline group (DOX, n = 6), received 5 mg/b.w.(kg)/day doxycycline without ISO treatment. In the ISO–treated groups, 24 hours after the second injection the surviving animals were randomly assigned to receive either doxycycline (5 mg/b.w(kg)/day or tap water. At the end of the 8 week long treatment period, body weights were measured, animals were sacrificed and the hearts were removed. The atria and great vessels were trimmed from the ventricles and the weight of the ventricles was measured and

normalized to body mass and tibia length. The ventricles were fixed in 10% formalin for histology or freeze clamped for Western blot analysis.

4.1.7 Determination of plasma B-type natriuretic peptide level

Blood samples were collected into Vacutainer tubes containing EDTA and aprotinin (0.6 IU/ml) and centrifuged at 1600 g for 15 minutes at 4°C to obtain plasma, which was collected and kept at -70°C. Plasma B-type natriuretic peptide-45 levels (BNP-45) were determined by enzyme immunoassay (BNP-45, Rat EIA Kit, Phoenix Pharmaceuticals Inc., CA, USA) (29).

4.1.8 Non-invasive evaluation of cardiac function

The investigators were blinded to the treatment protocol. Under baseline conditions, all animals were examined by means of echocardiography to exclude rats with any pre-existing heart abnormalities. Transthoracic two-dimensional echocardiography was performed under inhalation anesthesia at the beginning of the experiment and on final day, prior to sacrificing the animals. The rats were lightly anesthetized with a mixture of 1.5% isoflurane and 98.5% oxygen. The chest of each animal was shaved, acoustic coupling gel was applied, and a warming pad was used to maintain normothermia. The animals were imaged in the left lateral position. Cardiac diameters and function were measured parasternal from the short- and long-axis views at the midpapillary level by using a VEVO 770 high-resolution ultrasound imaging system (VisualSonics, Toronto, Canada), which was equipped with a 25 MHz transducer. Left ventricular (LV) systolic function (ejection fraction-EF), LV end-diastolic volume (LVEDV), LV end-systolic volume (LVESV), as well as the thickness of the septum and posterior wall (PW) were determined. EF (%) was calculated as 100x[(LVEDV - LVESV)/ LVEDV] (29) and FS (%) was calculated as left ventricular end-diastolic diameter (LVEDD) minus lef ventricular end-systolic diameter (LVESD) over the LVEDD x 100.

4.1.9 Histology

After fixation in formalin, the ventricles were sliced and embedded in paraffin. Sections (5 μm thick) were cut serially from base to apex. Sections were stained with Masson's trichrome stain to detect interstitial fibrosis, and quantified by the NIH ImageJ image processing program via its color deconvolution plugin (29).

4.1.10 Nitrotyrosine immunohistochemical staining

We performed immunohistochemical staining for nitrotyrosine, a marker of nitrooxidative stress, using a previously described method (64). Extensively stained area was also quantified using the NIH ImageJ image processing program via its color deconvolution plugin.

4.1.11 Western blot analysis

Fifty milligrams of heart samples were homogenized in ice-cold Tris buffer (50 mmol/l, pH 8.0) containing 50 mM sodium vanadate and protease inhibitor cocktail (Sigma-Aldrich Co., Budapest, Hungary) and harvested in 2× concentrated SDS-polyacrylamide gel electrophoresis sample buffer. Proteins were separated on a 12% SDS-polyacrylamide gel and transferred to nitrocellulose membranes. After blocking (2 h with 3% nonfat milk in Tris-buffered saline), membranes were probed overnight at 4 °C with antibodies recognizing the following antigens: mitofusin-2 (Mfn-2; 80 kDa; 1:1000; Cell Signaling), optic atrophy protein-1 (OPA-1; 100-110 kDa, 1:1000; Abcam), Drp-1 and phospho-specific Drp-1 Ser^{616} (95 kDa; 1:1000, Cell Signaling). Membranes were washed six times for 5 min in Tris-buffered saline (pH 7.5) containing 0.2% Tween (TBST) before addition of goat anti-rabbit horseradish peroxidase-conjugated secondary antibody (1:3000 dilution; Bio-Rad, Budapest, Hungary). Membranes were washed six times for 5 min in TBST and the antibody–antigen complexes were visualized by means of enhanced chemiluminescence. The results of Western blots were quantified using the NIH ImageJ program.

4.1.12 Statistical analysis

Statistical analysis was performed by analysis of variance and all of the data were expressed as the mean ± SEM. The homogeneity of the groups was tested by F-test (Levene's test). There were no significant differences among the groups. Comparisons among groups were performed using one-way ANOVA followed by Bonferroni correction in SPSS for Windows, version 21.0. All data are expressed as mean ± S.E.M. A value of $p < 0.05$ was considered statistically significant.

4.2 Results

4.2.1 Protective effect of doxycycline against the free radical–induced injury of cardiomyocytes

H9c2 cardiomyocytes were exposed to different concentrations of H_2O_2 for 24 hours. Fifty percent of myocyte cell death was detected at a concentration of 0.3 mM H_2O_2. Increasing concentrations of DOX (50 nM, 100 nM, 300 nM, 1 μM, 10μM) were able to significantly improve cell survival ($P < 0.01$; Fig 2).

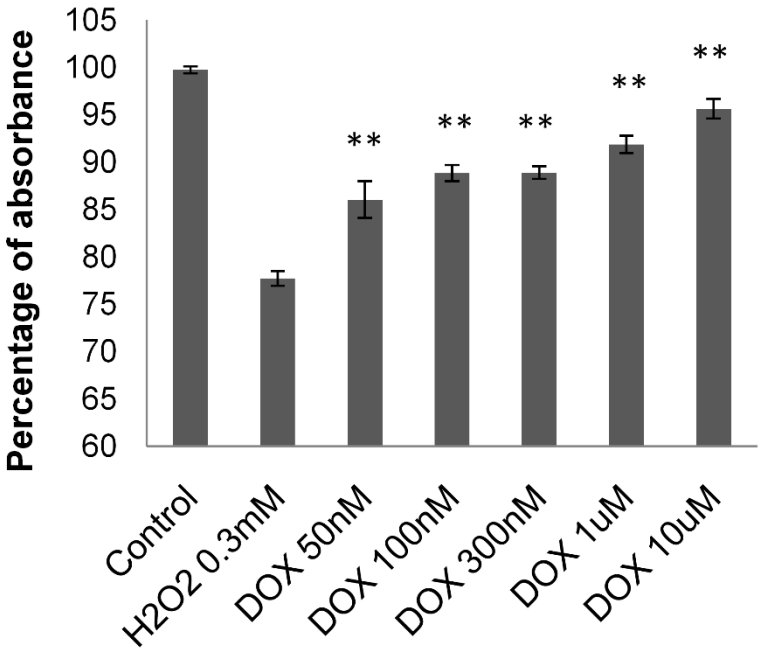

Fig 2. DOX protects against the H_2O_2–induced cell death

A wide range of doxycycline concentrations (50 nM, 100 nM, 300 nM, 1 μM, 10 μM) were applied to H_2O_2 – stressed (0.3 mM, 3h) H9c2 cells. All concentrations of DOX significantly improved the cell viability (**P < 0.01).

4.2.2 Doxycycline attenuates oxidative stress–induced mitochondrial fragmentation

Hydrogen peroxide induces mitochondrial fission resulting in fragmented mitochondria within 4 to 6 hours. This can be detected with MitoTracker dyes, or mitochondria–directed fluorescent proteins. The effect of doxycycline on hydrogen peroxide–induced mitochondrial fragmentation was analyzed by labeling the mitochondria with mitochondria–directed Advanced Red Fluorescent Protein (mARFP). Mitochondrial fragmentation was induced in H9c2 cells after incubation with 400 μM H_2O_2 for 5 hours, at which time the mitochondrial filaments disappeared and fragmented mitochondria with lengths shorter than 2 μm were

observed instead. Doxycycline reduced ROS–induced mitochondrial fragmentation at a concentration of 5 μM ($P < 0.05$, C vs. H_2O_2 and $P < 0.05$, H_2O_2 vs. DOX+ H_2O_2; Fig 3A).

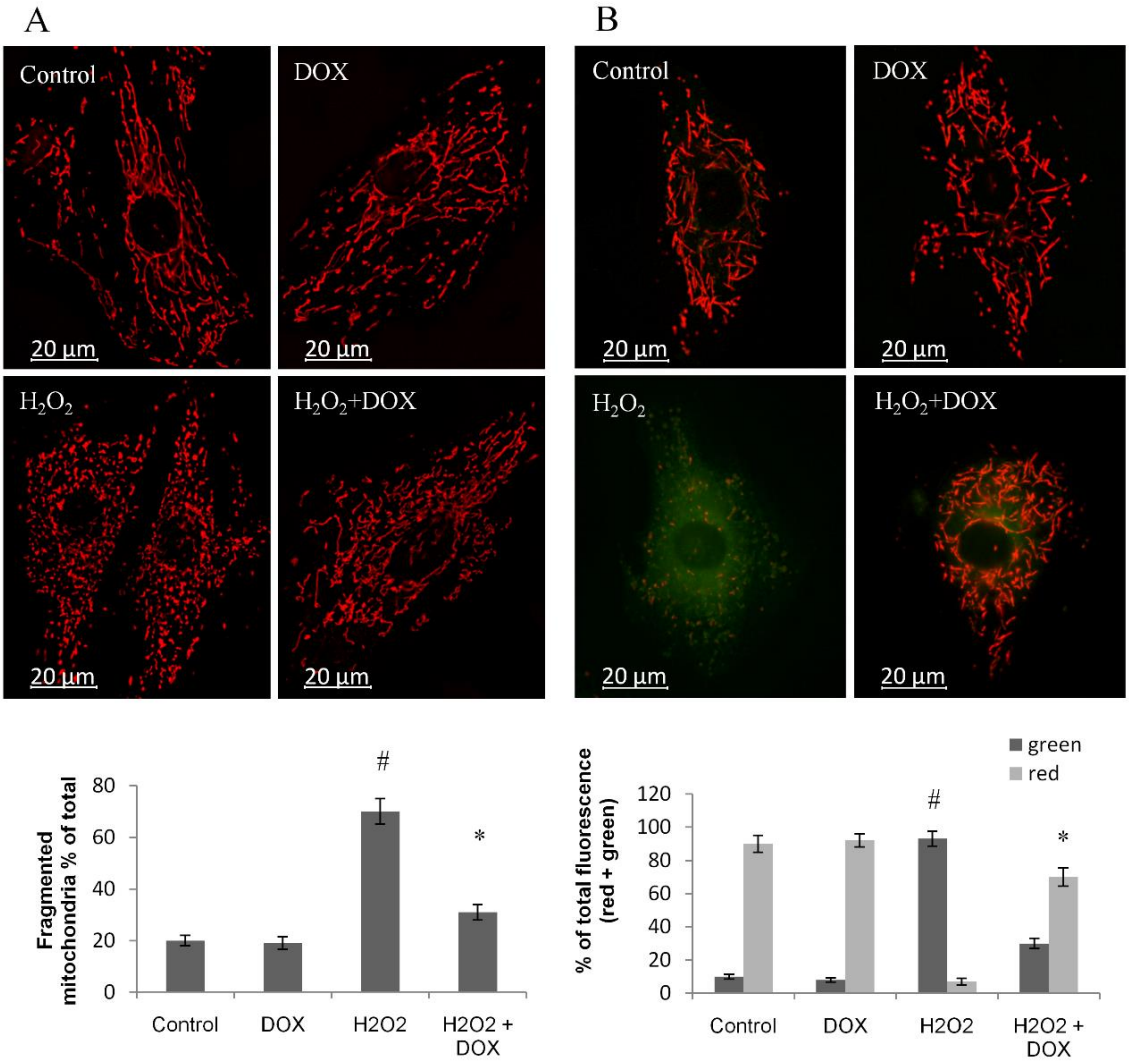

Fig 3. Mitochondrial depolarization and fragmentation in H9c2 cardiomyocytes.

(A) Mitochondrial fragmentation was induced in H9c2 cells after incubation with 400 μM H_2O_2 for 5 hours, at which time the mitochondrial filaments disappeared and fragmented mitochondria with lengths shorter than 2 μm were observed instead. Doxycycline reduced or completely prevented ROS–induced mitochondrial fragmentation at the concentration of 5 μM. **(B)** DOX protected H9c2 cells from cell death by preventing the depolarization of the mitochondrial membrane. Green and red fluorescence images of the same field were acquired using a fluorescent microscope equipped with a digital camera. The images were merged to demonstrate depolarization of Δψ in vivo, indicated by loss of the red component of the merged image. Some red fragments can also be seen,

representing the fragmented mitochondria. Representative merged images of three independent experiments are presented (#$P < 0.05$, C vs. H_2O_2 and *$P < 0.05$, H_2O_2 vs. DOX+H_2O_2).

4.2.3 Doxycycline hyperpolarizes the mitochondrial membrane of H9c2 cardiomyocytes

We studied the mitochondrial membrane potential of control, DOX (5 μM), H_2O_2 (400 μM), and H_2O_2+DOX–treated cells. After a 5 hour long treatment, cells were loaded with the voltage–sensitive fluorescent mitochondrial dye – JC1 – then red and green fluorescence was determined by fluorescent microscopy. DOX effectively prevented mitochondrial membrane depolarization ($P < 0.05$, C vs. H_2O_2 and $P < 0.05$, H_2O_2 vs. DOX+ H_2O_2; Fig 3B).

4.2.4 Doxycycline improves left ventricular function and moderates left ventricular hypertrophy in ISO treated rats

The echocardiographic parameters of animals did not differ significantly from each other at the beginning of the study. Heart rate did not differ significantly among the groups during the anesthesia. The thickness of the septum and posterior wall were also increased in the ISO group (indicating the presence of ventricular hypertrophy) compared to the control group ($P < 0.05$, ISO vs. C). Doxycycline treatment significantly reduced these unfavorable alterations. Systolic left ventricular function (EF %) and fractional shortening (FS %) were significantly lower in the ISO group ($P < 0.05$, ISO vs. C) and these deterioration was significantly improved by doxycycline administration ($P < 0.05$, ISO vs. ISO+DOX; Table 2; Fig 4).

Table 2. Effects of doxycycline on the echocardiographic parameters.

	Baseline	Control	DOX	ISO	ISO+DOX
EF (%)	76.42 ± 3.58	73.75 ± 1.39	72.81 ± 1.51	58.84 ± 1.27$^{\#}$	68.39 ± 0.94*
FS (%)	46.93 3.29	44.21 ± 1.41	43.62 ± 1.32	33.29 ± 0.19	39.96 ± 0.56*
Septum (mm)	1.52 ± 0.05	1.55 ± 0.04	1.46 ± 0.04	1.79 ± 0.08$^{\#}$	1.57 ± 0.04*
PW (mm)	1.50 ± 0.12	1.49 ± 0.74	1.42 ± 0.03	1.72 ± 0.05$^{\#}$	1.51 ± 0.04*
LVIDd (mm)	8.21 0.21	8.64 ± 0.29	8.30 ± 0.18	8.46± 0.07	8.31 ± 0.22
LVIDs (mm)	4.36 ± 0.33	4.77 ± 0.09	4.69 ± 0.19	5.34 ± 0.07$^{\#}$	4.84 ± 0.12*
LVEDV (ul)	365.83 ± 20.43	415.11 ± 32.63	375.50 ±17.64	371.34 ± 8.83	387.42 ± 22.42
LVESV (ul)	86.31 ± 15.86	107.52 ± 5.73	103.24 ± 9.85	147.16 ± 3.26$^{\#}$	121.42 ± 4.86*
LV mass (mg)	991.69 ± 58.51	989.30 ± 63.91	953.00 ± 21.05	1212.24 ± 48.30$^{\#}$	990.93 ± 59.33*

Control group (C) (n=5); doxycycline group (DOX) (n=6); isoproterenol group (ISO) (n=7); ISO+ doxycycline group (ISO+DOX) (n=7). EF: ejection fraction, FS: fractional shortening, PW: posterior wall, LVIDd: diastolic left-ventricular inner diameter, LVIDs: systolic left-ventricular inner diameter, LVEDV: left ventricular end-diastolic volume, LVESV: left-ventricular end-systolic volume, LV mass: calculated left vantricular mass. Values are mean ± S.E.M. #P < 0.05 vs. Control, *P < 0.05 vs. ISO.

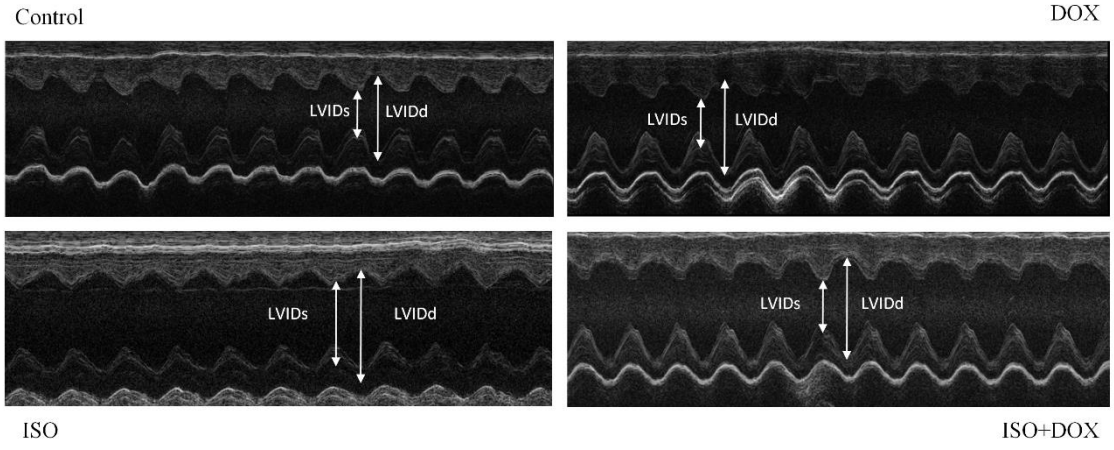

Fig 4. Representative echocardiographic M-mode images of left ventricles of control, DOX, ISO and ISO+DOX groups.

4.2.5 Doxycycline treatment improves the gravimetric parameters in an ISO–induced heart failure model

There was no significant difference in body weight between the groups at the beginning or the end of the experiment. Gravimetric measurements were performed and significantly elevated ventricular weight (WV, g, C: 1.27 ± 0.02; DOX: 1.28 ± 0.02; ISO: 1.46 ± 0.03; ISO+DOX: 1.31 ± 0.02; $P < 0.05$, C vs. ISO) as well as ventricular weight normalized to body weight (WV/BW, mg/g, C: 2.28 ± 0.12; DOX: 2.27 ± 0.09; ISO: 2.87 ± 0.13; ISO+DOX: 2.39 ± 0.06; $P < 0.05$, C vs. ISO) and to tibia length (TL) (WV/TL, mg/mm, C: 25.54 ± 0.28; DOX: 26.51 ± 0.69; ISO: 29.95 ± 0.47; ISO+DOX: 26.66 ± 0.92; $P < 0.05$, C vs. ISO) were detected. Doxycycline treatment prevented the unfavorable changes in gravimetric parameters in the ISO+DOX group ($P < 0.05$, ISO+DOX vs. ISO) (Table 3).

Table 3. Effect of doxycycline on the ventricular weight/tibia length (VW/TL) ratio and on plasma BNP.

Group	Control	DOX	ISO	ISO+DOX
Weight (g)	564.20 ± 21.55	569.67 ± 23.04	515.71 ± 19.66	550.86 ± 14.89
Ventricular weight (g)	1.27 ± 0.02	1.28 ± 0.02	1.46 ± 0.03$^{\#}$	1.31 ± 0.02*
Tibia length (mm)	48.00 ± 0.55	48.50 ± 0.76	48.86 ± 0.51	49.43 ± 0.49
Ventricular weight/body weight (mg/g)	2.28 ± 0.12	2.27 ± 0.09	2.87 ± 0.13	2.39 ± 0.06*
Ventricular weight/tibia length (mg/mm)	25.54 ± 0.28	26.51 ± 0.69	29.95 ± 0.47$^{\#}$	26.6 ± 0.92*
p-BNP (ng/ml)	1.62 ± 0.11	1.61 ± 0.01	2.29 ± 0.06$^{\#}$	1.66 ± 0.10*

(#$P < 0.05$ vs. control, *$P < 0.05$ vs. ISO)

Eight weeks after ISO–induced myocardial infarction, body weight, mass of ventricles and tibia length were measured. Ventricular weight/body weight (mg/g) and ventricular weight/tibia length (mg/mm) ratios were calculated. Plasma B-type Natriuretic Pepetide (p-BNP) level was determined by ELISA. Control group (C) (n=5); doxycycline group (DOX) (n=6); isoproterenol group (ISO) (n=7); ISO+ doxycycline group (ISO+DOX) (n=7). The results were expressed as mean ± S.E.M. #$P < 0.05$ vs. Control, *$P < 0.05$ vs. ISO.

4.2.6 Doxycycline inhibits the heart failure–induced elevation of plasma BNP level

Elevation in plasma BNP levels was strongly associated with the severity of heart failure. The BNP level increased significantly in the ISO group 8 weeks after myocardial infarction ($P <$

0.05, C vs. ISO). However, doxycycline could significantly reduce the plasma BNP level ($P < 0.05$, ISO vs. ISO+DOX) suggesting that doxycycline decreased the severity of postinfarction heart failure. There was no significant difference between the control and the DOX groups (Table 3).

4.2.7 Doxycycline decreases the interstitial collagen deposition in the myocardium

Histological analysis revealed marked scar tissue formation after ISO stress in failing rat hearts compared to the control group ($P < 0.05$). Doxycycline treatment significantly decreased the extent of interstitial fibrosis ($P < 0.05$). Doxycycline alone did not cause any alterations in myocardial hypertrophy or interstitial collagen deposition (Fig 5A).

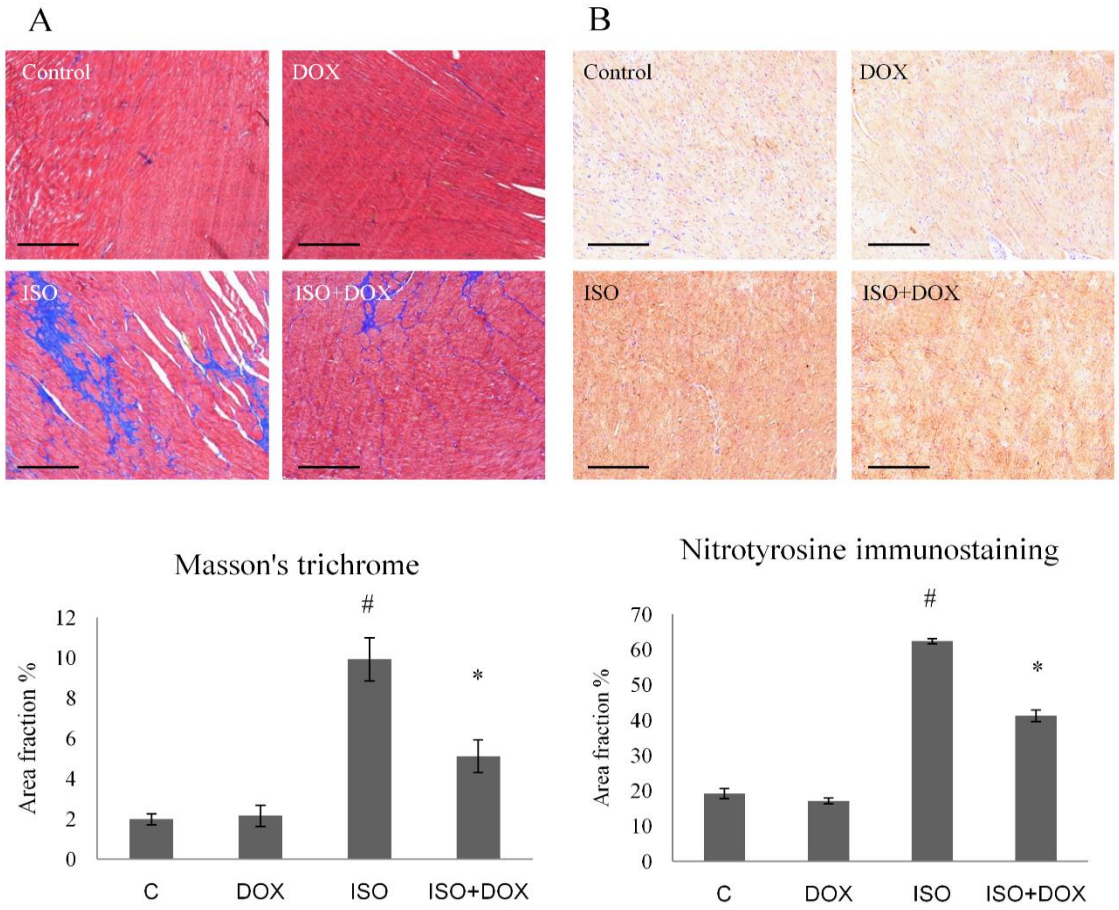

Fig 5. DOX reduces ISO–induced interstitial collagen deposition and protein nitrosylation in ISO–induced heart failure.

(A) Sections stained with Masson's trichrome (scale bar: 500μm, magnifications 5-fold). Control: age-matched rats, DOX: age-matched animals treated with doxycycline for 8 weeks, ISO: age-matched animals 8 weeks after ISO administration, ISO+DOX: age-matched animals treated with doxycycline, 8 weeks after ISO administration. Values are mean ± SEM. #P < 0.05 (ISO vs. control group), *P < 0.05 (ISO+DOX vs. ISO group). **(B)** Representative immunohistochemical stainings for nitrotyrosine (NT, brown staining, scale bar: 500μm, magnifications 5-fold) in the myocardium of control: age-matched rats, DOX: age-matched animals treated with doxycycline for 8 weeks, ISO: age-matched animals 8 weeks after ISO administration, ISO+DOX: age-matched animals treated with doxycycline, 8 weeks after ISO administration. Values are mean ± SEM. #P < 0.05 (ISO vs. control group), *P < 0.05 (ISO+DOX vs. ISO group).

4.2.8 Effects of doxycycline on the oxidative stress marker nitrotyrosine

The presence of oxidative stress was been confirmed in our rodent heart failure model by the investigation of a lipid peroxidation product, NT. Myocardial sections from the control group showed almost no immunostaining for NT. In contrast, in animals with heart failure (ISO), immunostaining notably increased ($P < 0.05$, C vs. ISO), but this increase was attenuated by DOX treatment ($P < 0.05$, ISO vs. ISO+DOX; Fig 5B).

4.2.9 Effect of doxycycline on the expression of OPA-1 and Mfn-2 and phosphorylation of Drp-1^{Ser616}

OPA-1 expression significantly increased in the DOX treated groups compared to the control and ISO groups ($P < 0.05$, control vs. DOX and $P < 0.05$, ISO vs. ISO+DOX) whereas the expression of Mfn-2 decreased significantly in the ISO+DOX group compared to the ISO group ($P < 0.05$, ISO vs. ISO+DOX). The phosphorylation level of Drp-1^{Ser616} increased significantly in the ISO group and decreased significantly in the ISO+DOX group ($P < 0.05$, C vs. ISO and $P < 0.05$, ISO vs. ISO+DOX). Protein levels were measured with Nanodrop and GAPDH was used as loading control (Fig 6).

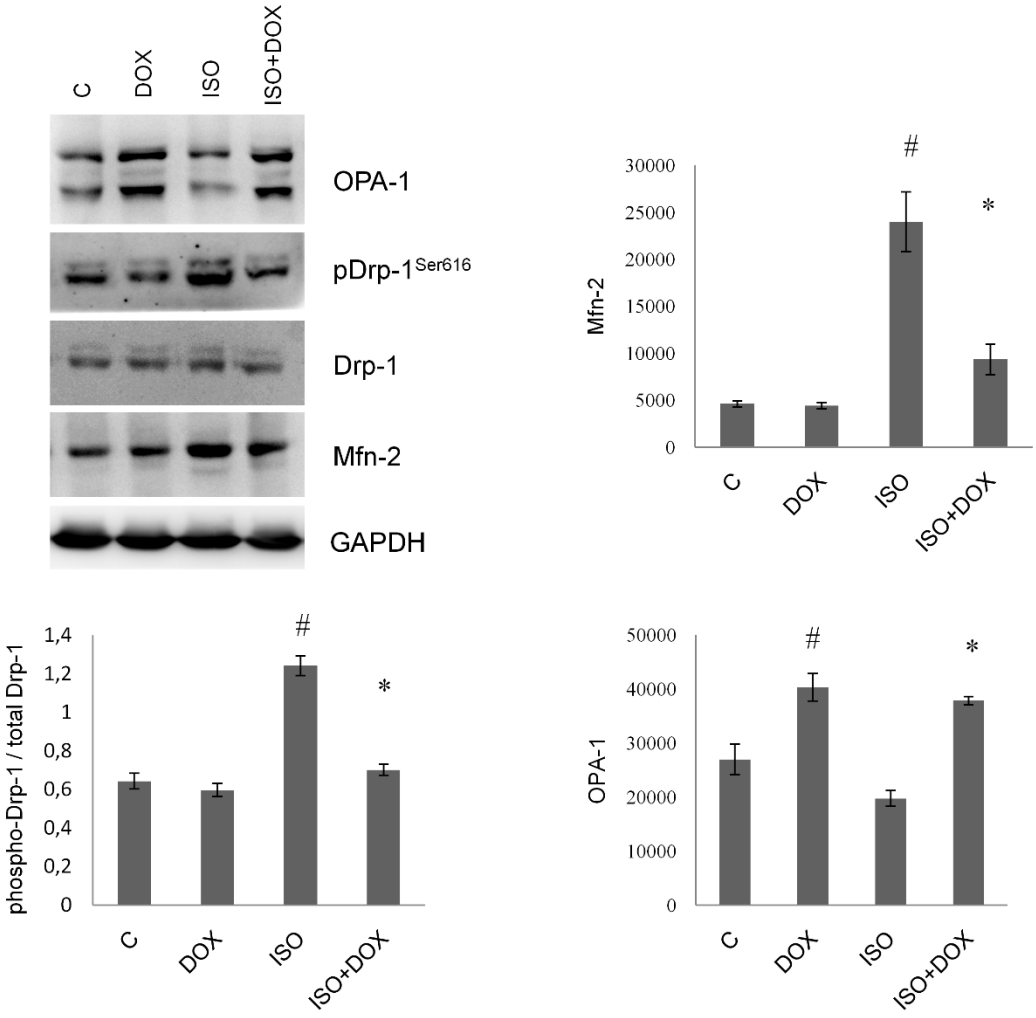

Fig 6. DOX favorably modulates the expression of Mfn-2, OPA-1 and the phosphorylation of Drp-1.
Representative western blot analysis of Mfn-2, OPA-1, Drp-1 and pDrp-1^{Ser616} and densitometric evaluation is shown. PhosphoDrp-1^{Ser616} bands were normalized to the appropriate Drp-1 bands. Representative blots and bar diagrams of three independent experiments are presented. C: control animals, ISO: animals 8 weeks after ISO administration; ISO + DOX: animals treated with doxycycline, 8 weeks after ISO administration; DOX: animals treated with doxycycline for 8 weeks. Values are mean ± SEM. # $P < 0.05$ vs control, *$P < 0.05$ vs. ISO.

4.3 Discussion

We investigated the effect of DOX on H9c2 cardiomyocyte cell culture and on an isoproterenol–induced heart failure animal model. Subcutaneous administration of isoproterenol produces diffuse myocardial necrosis predominantly subendocardially (28, 65).

The significant myocardial cell loss is followed by hypertrophy and remodeling leading to impaired left ventricular function and heart failure similar to that observed in post-MI patients. LV systolic function is a strong predictor of cardiac mortality and morbidity (66). ISO treatment significantly decreased the systolic left ventricular function, elevated ventricular wall thickness and diameter and caused significant myocyte hypertrophy. DOX was capable of preserving LV systolic function (EF%, FS%) and normalized wall thickness and ventricular diameter (Table 2, Fig 4). In accordance with these results, plasma BNP levels increased in the ISO–treated animals, and this increase was attenuated by DOX treatment (Table 3). There are data in the literature about the protective effect of doxycycline on isoproterenol induced cardiac hypertrophy and on the early phase of remodeling (36, 37). Our working group verified for the first time that DOX strikingly reduces the severity of postinfarction heart failure in an advanced stage.

Our histological examinations showed that ISO treatment induced excessive fibrosis, which was highly reduced by DOX treatment (Fig 5A). This effect is presumably based on its matrix metalloproteinase inhibition which has been described previously (67, 68). The effect of DOX was so prominent in our animal model, that we wanted to further clarify its action on myocardial protection.

Recently emerging evidence indicates that myocardial oxidative stress contributes to heart failure (69, 70). To establish the presence of oxidative damage in our animal model, we performed nitrotyrosine immunohistochemical analysis on the rat heart samples. Rats treated with ISO showed increased ROS production, which was highly attenuated by DOX treatment (Fig 5B).

There are some data in the literature about the antioxidant and scavenging properties of doxycycline (71). Doxycycline has a multiple-substituted phenol ring which is the key to its ROS-scavenging abilities. The reaction of the phenol ring with a free radical generates a phenolic radical that becomes relatively stable and unreactive (72). It is also supposed that doxycycline may inhibit MMPs by attenuating the oxidative stress (73).

Since mitochondria are a major source (and target) of ROS and play a critical role in energy production, we turned our attention to these organelles. Intensive research on the mitochondria has previously demonstrated that their structural and functional integrity is essential for maintaining normal myocardial function (8). The tightly controlled balance between mitochondrial fusion and fission is important in high energy demanding cells, such as cardiomyocytes. Defects in mitochondrial dynamics have been associated with various disorders, including heart failure, ischemia/reperfusion injury, diabetes, and aging (13). We first

tested the effect of DOX on a H9c2 cardiomyocyte cell culture, where DOX protected cardiomyocytes against oxidative injury in the SRB assay (Fig 2). Next we examined the effect of DOX on ROS–induced mitochondrial fragmentation and membrane potential. Our results showed that DOX protected mitochondria against ROS–induced mitochondrial fragmentation (Fig 3A) and prevented ROS–induced collapse of the mitochondrial membrane potential (Fig 3B), processes that cause rapid impairment of mitochondrial and cellular function leading to necrotic and apoptotic cell death (74-76).

We further investigated the effect of DOX on the expression of dynamin-like GTPases (OPA-1, Mfn-2, DRP-1) responsible for mitochondrial dynamics in western blot analysis of rat heart samples. It has been reported that Mfn-2 is markedly induced by oxidative stress in H9c2 cardiomyocytes and Mfn-2 creates physical connection between mitochondria and endoplasmic reticulum (17). After mitochondria is connected to the endoplasmic reticulum, a high amount of calcium enters the mitochondria from the ER and induces mitochondrial fragmentation (18, 77) (Fig.1). It is also known that elevated steady state level of OPA-1 leads to mitochondrial fusion and improves cell survival. On the contrary DRP-1 phosphorylation on Ser616 leads to mitochondrial fragmentation. It was reported earlier that pharmacological inhibition of Drp-1 attenuates mitochondrial membrane depolarization and protects the heart from ichemia/reperfusion injury, and Drp-1 expression is reduced in Mfn-2 knockout hearts (16, 19). Reduced expression of Mfn-2 makes mitochondria more tolerant to oxidative stress and Ca^{2+} overload (17). In our animal model, ISO treatment decreased OPA-1 and increased Mfn-2 levels, and augmented the phosphorylation of Drp-1. DOX was able to favorably modulate the steady state level of OPA-1, Mfn-2 and the phosphorylation of Drp-1, which prevented mitochondrial fragmentation and improved cell survival (Fig 6).

Some mitochondria targeted drugs such as PT pore inhibitors, NO analogs, antioxidants, potassium channel openers, metabolic modulators, have been examined in various clinical trials (9, 78). Unfortunately, many of these drugs have failed, while others are still under investigation (79, 80), showing that effective modification of this fine balance in mitochondrial metabolism is difficult.

According to our results, DOX might be a promising agent in the treatment of postinfarction heart failure. Besides its well-known protective effect on cardiac hypertrophy, remodeling and fibrosis, we could demonstrate that DOX was able to decrease the ROS-induced mitochondrial fragmentation and depolarisation on H9C2 cardiomyocytes, and beneficially modulated the steady state level of OPA-1, Mfn-2 and the phosphorylation of Drp-1 in our postinfarction heart

failure model. Further investigations are needed to better understand its protective effect on mitochondrial metabolism, ROS production and cell survival.

5 Examination of resveratrol in a postinfarction heart failure model

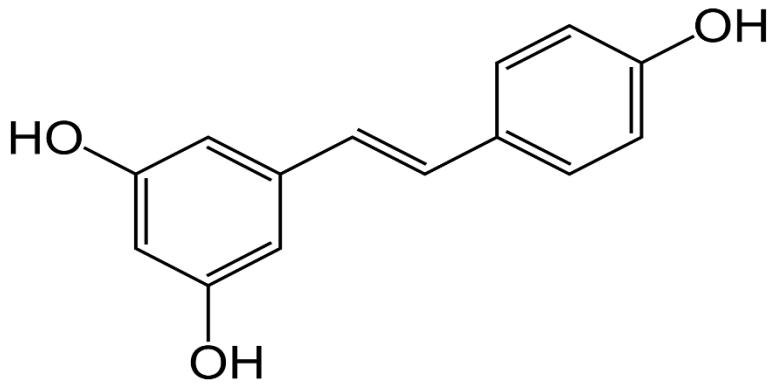

Fig 7. Chemical structure of resveratrol (RES).

5.1 Methods

5.1.1 Experimental protocol

Male 20-week-old Wistar rats (410–480 g) were used for the experiments. Animals received care according to the Guide for the Care and Use of Laboratory Animals published by the US National Institute of Health (NIH Publication No. 85-23, revised 1996) and the experiment was approved by the Animal Research Review Committee of the University of Pecs, Medical School (Permit number: BA02/2000-2/2010). The animals were housed under standardized conditions, 12 h dark–light cycle in solid bottomed polypropylene cages, and received commercial rat chew *ad libitum*. RES or clean water was administered as drink *ad libitum* for 8 weeks. We set the dosage of resveratrol to 15 mg/kg/day (61, 81, 82).

The rats were treated twice on two consecutive days with 80 mg/kg ISO (Sigma-Aldrich) or vehicle subcutaneously to induce postinfarction remodeling as previously described. The animals were divided into four groups: Control group (C), received clear water without ISO treatment; the second group of rats received two subcutaneous injections of isoproterenol at the dosage of 80 mg/kg (ISO); ISO + RES group (ISO+RES), received resveratrol with ISO treatment; resveratrol group (RES), received resveratrol without ISO treatment. RES inhibitor

treatment was delayed 24 h to avoid suppression of infarct size. At the end of the 8-week-long period, body weights were measured, animals were sacrificed and the hearts were removed. Atria and great vessels were trimmed from ventricles; the weight of the ventricles was measured and normalized to body mass. Afterwards, ventricles were fixed in 10% formalin for histology or freeze clamped for Western blot analysis.

5.1.2 Isoproterenol heart failure model

For both experimental protocol we used the ISO-induced myocardial infarct model that is a relevant murine model of postinfarction heart failure. Subcutaneous administration of isoproterenol produces patchy myocardial necrosis predominantly subendocardially. The significant myocardial cell loss is followed by consequent left ventricular hypertrophy and cardiac fibrosis, the left ventricular function decreases and myocardial remodeling occurs. Eventually these processes are leading to heart failure similar to the one obeserved in post-MI patients. Because isoproterenol is rapidly metabolized, acute adverse effects of the drug can be avoided.

5.1.3 Noninvasive evaluation of cardiac structure and function

Under baseline conditions, all animals were examined by means of echocardiography to exclude rats with any heart abnormalities. Transthoracic echocardiography was performed under inhalation anaesthesia at the beginning of the experiment and on the day of sacrifice. The rats were lightly anaesthetized with a mixture of 1.5% isoflurane and 98.5% oxygen. The chest of the animals was shaved, acoustic coupling gel was applied, and a warming pad was used to maintain normothermia. The animals were imaged in the left lateral position. Cardiac diameter and functions were measured from short- and long-axis views at the mid-papillary level using a VEVO 770 high-resolution ultrasound imaging system (VisualSonics, Toronto, Canada), which is equipped with a 25-MHz transducer. The investigators were blinded to the treatment protocol. Left ventricular (LV), ejection fraction (EF), LV end-diastolic volume, LV end-systolic volume, and the thickness of the septum and posterior wall were determined. EF (percentage) was calculated by 100 x [(LVEDV - LVESV)/LVEDV]. (29).

5.1.4 Histology

For histologic examnination ventricles were fixed in formalin and sliced and embedded in paraffin. Sections (5-μm thick) were cut serially from base to apex. LV sections were stained with Masson's trichrome to detect the interstitial fibrosis, and quantified by the NIH ImageJ image processing program via its colour deconvolution plugin (29).

5.1.5 Nitrotyrosine immunohistochemical staining

We performed immunohistochemical staining for nitrotyrosine, a nitro-oxidative stress-marker, using a previously described method. Extensively stained areas were also quantified using the NIH ImageJ image processing program via its colour deconvolution plugin (64).

5.1.6 Determination of plasma B-type natriuretic peptide level

Blood samples were collected into Vacutainer tubes containing EDTA and aprotinin (0.6 IU/ml) and centrifuged at 1600 g for 15 minutes at 4°C to obtain plasma, which was collected and kept at -70°C. Plasma B-type natriuretic peptide-45 levels (BNP-45) were determined by enzyme immunoassay method (BNP-45, Rat EIA Kit, Phoenix Pharmaceuticals Inc., CA, USA) (29).

5.1.7 Western blot analysis

Fifty milligrams of heart samples were homogenized in ice-cold Tris buffer (50 mmol/l, pH 8.0) containing 50 mM sodium vanadate and protease inhibitor cocktail (Sigma-Aldrich Co., Budapest, Hungary) and harvested in 2× concentrated SDS-polyacrylamide gel electrophoresis sample buffer. Proteins were separated on 12% SDS-polyacrylamide gel and transferred to nitrocellulose membranes. After blocking (2 h with 3% nonfat milk in Tris-buffered saline), membranes were probed overnight at 4 °C with antibodies recognizing the following antigens: phospho-specific mitogen-activated protein (MAP) kinase phosphatase-1 (*MKP-1*) Ser359 (1:1000), phospho-specific Akt-1/protein kinase B-α Ser473 (1:1000), phosphospecific glycogen synthase kinase (GSK)-3β Ser9 (1:1000), phospho-specific p38 mitogenactivated protein kinase (p38-MAPK) Thr180–Gly–Tyr182 (1:1000), ERK1/2$^{Thr183\text{-}Tyr185}$, COX-2 (1:1000), and iNOS (1:1000). Membranes were washed six times for 5 min in Tris-buffered saline (pH 7.5) containing 0.2% Tween (TBST) before the addition of goat anti-rabbit horseradish peroxidase-conjugated secondary antibody (1:3000 dilution; Bio-Rad, Budapest, Hungary). Membranes were washed six times for 5 min in TBST and the antibody–antigen

complexes were visualized by means of enhanced chemiluminescence. The results of Western blots were quantified using the NIH ImageJ program.

5.1.8 Statistical analysis

Statistical analysis was performed by analysis of variance and all of the data were expressed as the mean ± SEM. The homogeneity of the groups was tested by F-test (Levene's test). There were no significant differences among the groups. Comparisons among groups were made by one-way ANOVA followed by Bonferroni correction or Tukey HSD's post hoc tests in SPSS for Windows, version 21.0. All data are expressed as mean ± S.E.M. A value of $p<0.05$ was considered statistically significant.

5.2 Results

5.2.1 Resveratrol treatment improved the gravimetric parameters in ISO-induced heart failure model

Body weights did not differ significantly among the four groups at the beginning or the end of the experiment. Gravimetric measurements were performed and significantly elevated ventricular weight (WV, g) (C: 1.33±0.01; RES: 1.31±0.01; ISO: 1.53±0.02; ISO+RES: 1.35±0.01) (C vs. ISO $P<0.05$) as well as ventricular weight normalized to body weight (WV/BW, mg/g) (C: 2.25±0.06; RES: 2.21±0.08; ISO: 2.81±0.06; ISO+RES: 2.29±0.09) (C vs. ISO $P < 0.05$) and to tibia length (TL) (WV/TL, mg/mm) (C: 26.03±0.47; RES: 25.33±0.33; ISO: 29.96±0.28; ISO+RES: 27.02±0.13) (C vs. ISO $P<0.05$) were detected. Resveratrol treatment prevented the unfavourable changes in gravimetric parameters indicating hypertrophy in the ISO+RES group (ISO+RES vs. ISO $p<0.05$). (Table 4).

Table 4. Effects of RES and ISO on the gravimetric parameters.

Group	Control	RES	ISO	ISO+RES
weight (g)	595.86±15.15	596.00±21.30	544.50±11.63	593.86±18.41
ventricular weight (g)	1.33±0.01	1.31±0.01	1.53±0.02#	1.35±0.01*
tibia length (mm)	51.43±0.72	51.57±0.72	50.86±0.55	49.86±0.35
ventricular weight/body weight (mg/g)	2.25±0.06	2.21±0.08	2.81±0.06#	2.29±0.09*
ventricular weight/tibia length (mg/mm)	26.03±0.47	25.33±0.33	29.96±0.28#	27.02±0.13*

Eight weeks after ISO-induced myocardial infarction, body weight, mass of ventricles and tibia length were measured. Ventricular weight/body weight (mg/g) and ventricular weight/tibia length (mg/mm) ratios were calculated. The results are expressed as mean±S.E.M. #P<0.05 vs. Control. *P<0.05 vs. ISO.

5.2.2 Resveratrol decreased the heart failure-induced elevation of plasma BNP level

ISO administration led to a significant increase in BNP level in the ISO group 8 weeks after myocardial infarction in our study (C vs. ISO P<0.05). However resveratrol significantly attenuated this response (ISO+RES vs. ISO P<0.05) suggesting that resveratrol decreases the severity of postinfarction heart failure. There was no significant difference between the C and the RES groups (Fig. 8) .

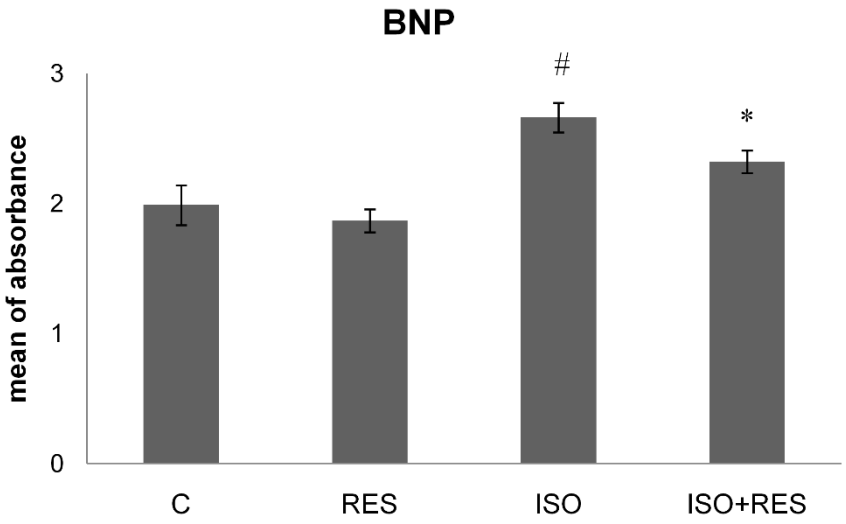

Fig 8. RES inhibited the heart failure-induced elevation of plasma BNP level. Plasma BNP level was determined using an ELISA method as described in the Materials and methods. C: control animals; RES: animals

treated with resveratrol for 8 weeks; ISO: animals 8 weeks after ISO administration; ISO + RES: animals treated with resveratrol, 8 weeks after ISO administration. Values are mean ± SEM, ∗P<0.05 vs. ISO, #P<0.05 vs C.

5.2.3 Resveratrol improved left ventricular function and moderated left ventricular hypertrophy in ISO-treated rats

The echocardiographic parameters of animals did not differ significantly from each other at the beginning of the study. Heart rate did not differ significantly during anaesthesia among the groups. LVESV and LVIDs were significantly higher in the ISO group (ISO vs. C and ISO vs. RES $p<0.05$). The thickness of the septum and posterior wall and calculated LV mass were also higher in the ISO group (indicating the presence of ventricular hypertrophy) compared to the control group (ISO vs. C $p<0.05$). Resveratrol treatment significantly reduced these unfavourable alterations. Systolic left ventricular function (EF %) were significantly lower in the ISO group (ISO vs. C $p<0.05$) and this deterioration was significantly improved by resveratrol administration (ISO vs. ISO+RES, $p<0.05$) (Table 5, Fig. 9).

	Baseline	**C**	**RES**	**ISO**	**ISO+RES**
EF (%)	75.62±0.87	71.70±1.61	72.47±1.69	56.96±1.43$^{\#}$	67.49±1.14*
Septum (mm)	1.63±0.05	1.65±0.10	1.61±0.03	1.82±0.03$^{\#}$	1.70±0.02*
PW (mm)	1.57±0.03	1.59±0.07	1.59±0.03	1.81±0.06$^{\#}$	1.60±0.02*
LVIDd (mm)	8.19±0.11	8.44±0.22	8.43±0.17	7.88±0.12	8.41±0.23
LVIDs (mm)	4.42±0.08	4.85±0.09	4.69±0.19	5.70±0.2$^{\#}$	4.90±0.12*
LVEDV (µl)	364.23±10.38	393.36±19.32	386.40±16.82	365.54±6.64	401.59±18.63
LVESV (µl)	88.83±4.40	109.9±4.53	106.14±7.26	157.71±7.29$^{\#}$	130.27±6.69*
LV mass (mg)	994.1±21.8	1035.31±59.79	1038.38±44.44	1239.14±76.5$^{\#}$	1041.85±35.50*

Table 5. Resveratrol improved left ventricular function in ISO-treated rats and reduced left ventricular hypertrophy Control group (C); resveratrol group (RES); isoproterenol-treated group: (ISO); ISO+ resveratrol group (ISO+RES). EF: ejection fraction, LVESV: left-ventricular end-systolic volume, LVEDV: left ventricular end-diastolic volume, LVIDd: diastolic left ventricular inner diameter, LVIDs: systolic left-ventricular inner diameter.

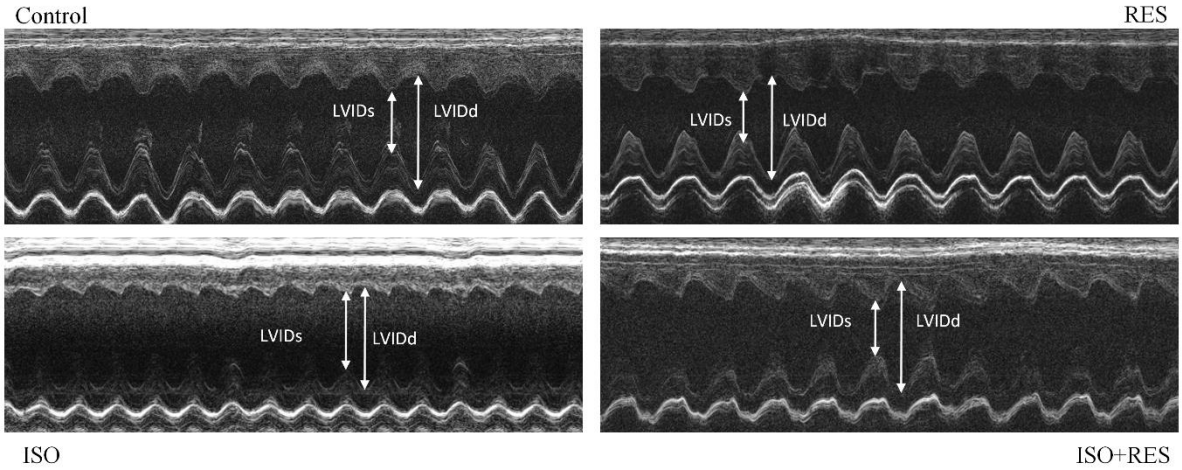

Fig 9. Representative echocardiographic M-mode images of left ventricles of animals from Control, RES, ISO and ISO+RES groups.

5.2.4 Resveratrol decreased interstitial collagen deposition in the myocardium

Marked scar tissue formation was revealed by histological analysis after ISO stress in failing rat hearts compared to the control group ($P<0.05$). Resveratrol treatment significantly decreased the extent of interstitial fibrosis ($P<0.05$). Resveratrol alone did not cause any significant alterations in physiological conditions related to myocardial hypertrophy or interstitial collagen deposition (Fig 10A).

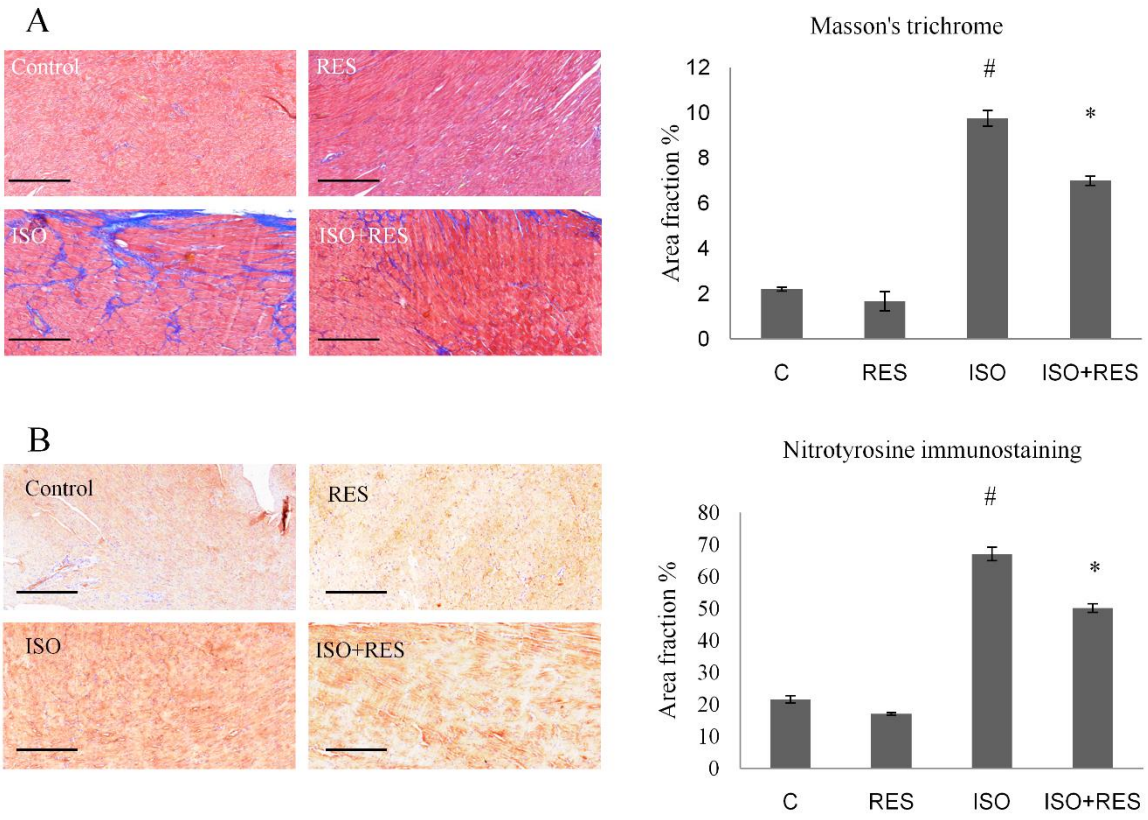

Fig 10. RES treatment moderated ISO-induced interstitial collagen deposition and protein nitrosylation in ISO-induced heart failure. (A) Representative sections stained with Masson's trichrome, scale bar: 500 μm, magnifications 10-fold. Control: age-matched control rats. RES: age-matched animals treated with resveratrol for 8 weeks. ISO: age-matched animals 8 weeks after ISO administration; ISO+RES: age-matched animals treated with resveratrol, 8 weeks after ISO administration. Values are mean ± SEM, P<0.05 (ISO vs. Control group), P<0.05 (ISO+RES vs. ISO group). **(B)** Representative immunohistochemical stainings for nitrotyrosine (NT, brown staining, scale bar: 500 μm, 10x magnification) in the myocardium of: Control: age-matched control rats; RES: age-matched animals treated with resveratrol for 8 weeks; ISO: age-matched animals 8 weeks after ISO administration; ISO+RES: age-matched animals treated with resveratrol, 8 weeks after ISO administration. Values are mean ± SEM, #P<0.05 (ISO vs. Control group), *P<0.05 (ISO+RES vs. ISO group).

5.2.5 Effects of resveratrol on the oxidative stress marker nitrotyrosine

The presence of oxidative stress was confirmed in our rodent heart failure model by the measurement of NT, which is a product of tyrosine nitration. Almost no immunostaining for NT was observed in myocardial sections of the control group. In contrast, in animals with heart failure (ISO), immunostaining was significantly more extensive (P<0.05, C vs. ISO), but this increase was attenuated by RES treatment (P < 0.05, ISO vs. ISO+RES; Fig. 10B).

5.2.6 Resveratrol favourably influenced the phosphorylation of Akt-1^{Ser473}, GSK-3ß^{Ser9} in failing myocardium

The level of Akt-1^{Ser473} was significantly higher in the RES and ISO+RES groups compared to the control and ISO groups ($P<0.05$) respectively. Although the level of Akt-1^{Ser473} was significantly elevated in ISO-treated animals (ISO vs. C $P<0.05$), the highest activities were observed in the ISO+RES group (ISO vs. ISO+RES $P<0.05$). The level of GSK-3β^{Ser9} was also slightly elevated in the RES group compared to the control group and significantly decreased in ISO animals compared to control animals ($P<0.05$ C vs. ISO). The elevation in the ISO+RES group was significant compared to the ISO group too ($P<0.05$ ISO+RES vs. ISO) GAPDH was used as a loading control (Fig 11).

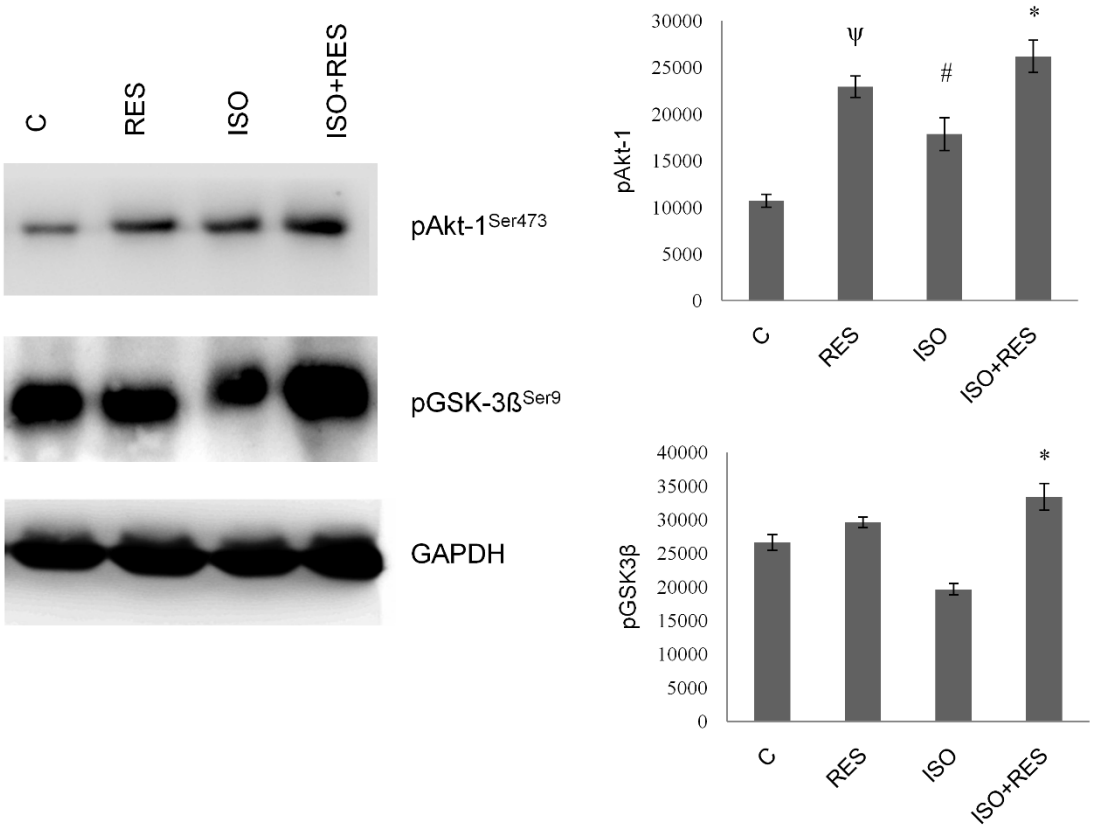

Fig 11. **Effect of resveratrol treatment on Akt-1^{Ser473}, GSK-3ß^{Ser9}.** Representative western blot analysis of Akt-1^{Ser473}/GSK-3ß^{Ser9} phosphorylation and densitometric evaluation is shown. GAPDH was used as a loading control. Representative blots and bar diagrams of three independent experiments are presented. C: control animals; RES: animals treated with resveratrol for 8 weeks; ISO: animals 8 weeks after ISO administration; ISO + RES: animals treated with resveratrol, 8 weeks after ISO administration. Values are mean ± SEM, #P <0.05 vs. Control, ∗P<0.05 vs. ISO, ψP<0.05 C vs. RES.

5.2.7 Resveratrol attenuated the phosphorylation of p38-MAPK$^{Thr180\text{-}Gly\text{-}Tyr182}$, ERK1/2$^{Thr183\text{-}Tyr185}$ and increased the amount of MKP-1 in ISO-stressed hearts

The level of phosphorylation of p38-MAPK$^{Thr180\text{-}Gly\text{-}Tyr182}$ and ERK1/2$^{Thr183\text{-}Tyr185}$ was significantly elevated in the ISO group compared to the control group (C vs. ISO P<0.05). There was a significant reduction in the phosphorylation level of p38-MAPK$^{Thr180\text{-}Gly\text{-}Tyr182}$ in the ISO+RES group versus the ISO group (P<0.05, ISO vs. ISO+RES). The activation of

ERK1/2$^{Thr183\text{-}Tyr185}$ was also significantly reduced in the ISO+RES group, compared to the ISO group (P<0.05, ISO vs. ISO+RES). Consequently the steady state amount of MKP-1 was significantly elevated in the ISO+RES group compared to the ISO group. Interestingly there was a strong and significant elevation in the RES group compared to the control group (P<0.05 C vs. RES). GAPDH was used as a loading control (Fig 12).

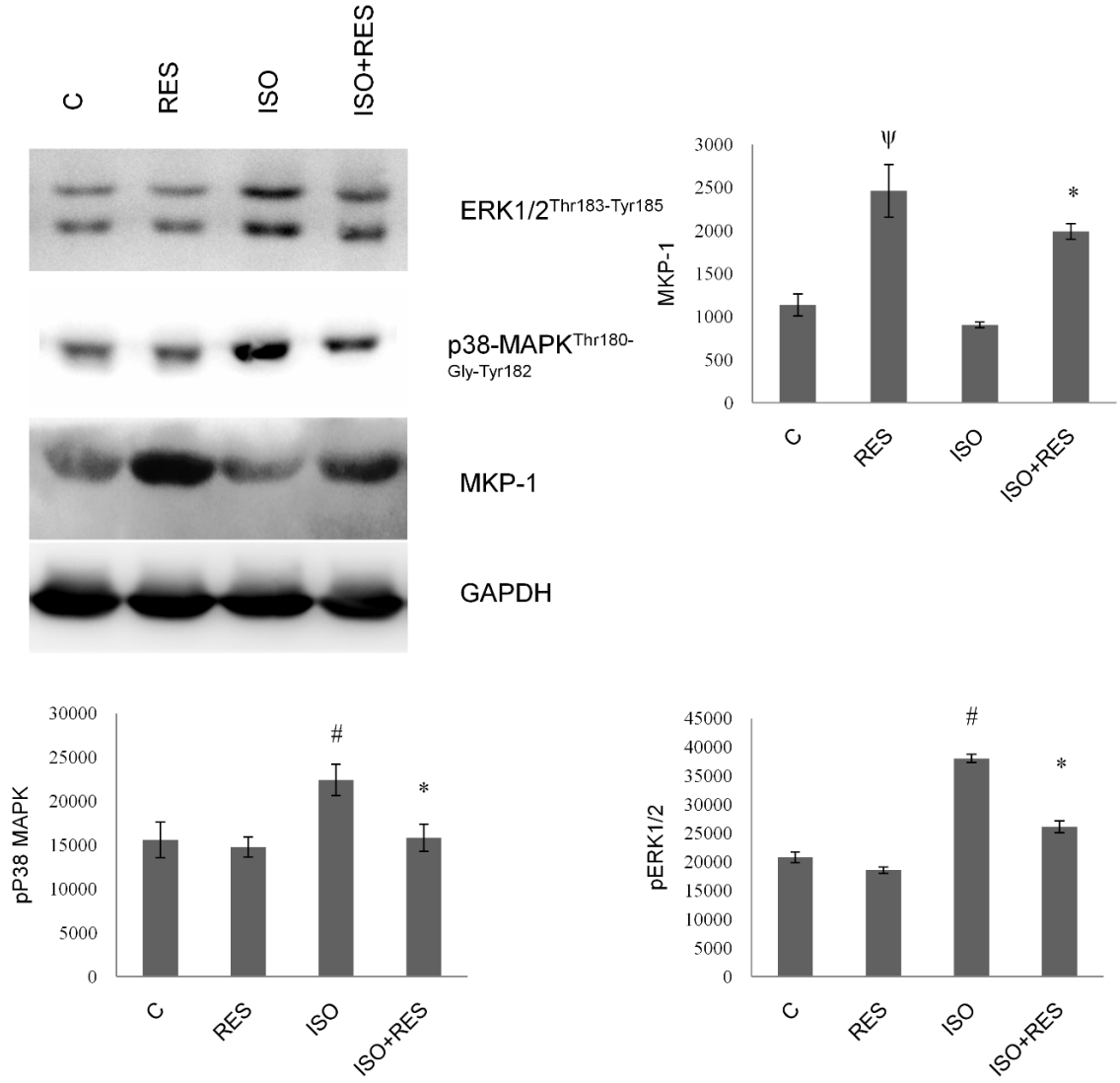

Fig 12. Effect of resveratrol treatment on the phosphorylation of p38-MAPK$^{Thr180\text{-}Gly\text{-}Tyr182}$, ERK1/2$^{Thr183\text{-}Tyr185}$ and on the amount of MKP-1. Representative western blot analysis of p38-MAPK$^{Thr180\text{-}Gly\text{-}Tyr182}$, ERK1/2 phosphorylation and MKP-1 level; a densitometric evaluation is shown. GAPDH was used as a loading control. Representative blots and bar diagrams of three independent experiments are presented. C: control animals; RES: animals treated with resveratrol for 8 weeks; ISO: animals 8 weeks after ISO administration; ISO + RES: animals treated with resveratrol, 8 weeks after ISO administration. Values are mean ± SEM, #P <0.05 Control vs. ISO, ψP<0.01 C vs. RES, ∗P<0.05 ISO vs. ISO+RES.

5.2.8 Resveratrol decreased the expression of COX-2 and iNOS

The expression of COX-2 and iNOS was significantly elevated in ISO compared to the control ($P<0.05$, C vs. ISO) and significantly decreased in ISO+RES compared to ISO ($P<0.05$, ISO vs. ISO+RES). Although the activation level of COX-2 was slightly decreased in RES compared to the control, the only significant difference was between ISO+RES and ISO. GAPDH was used as a loading control (Fig 13).

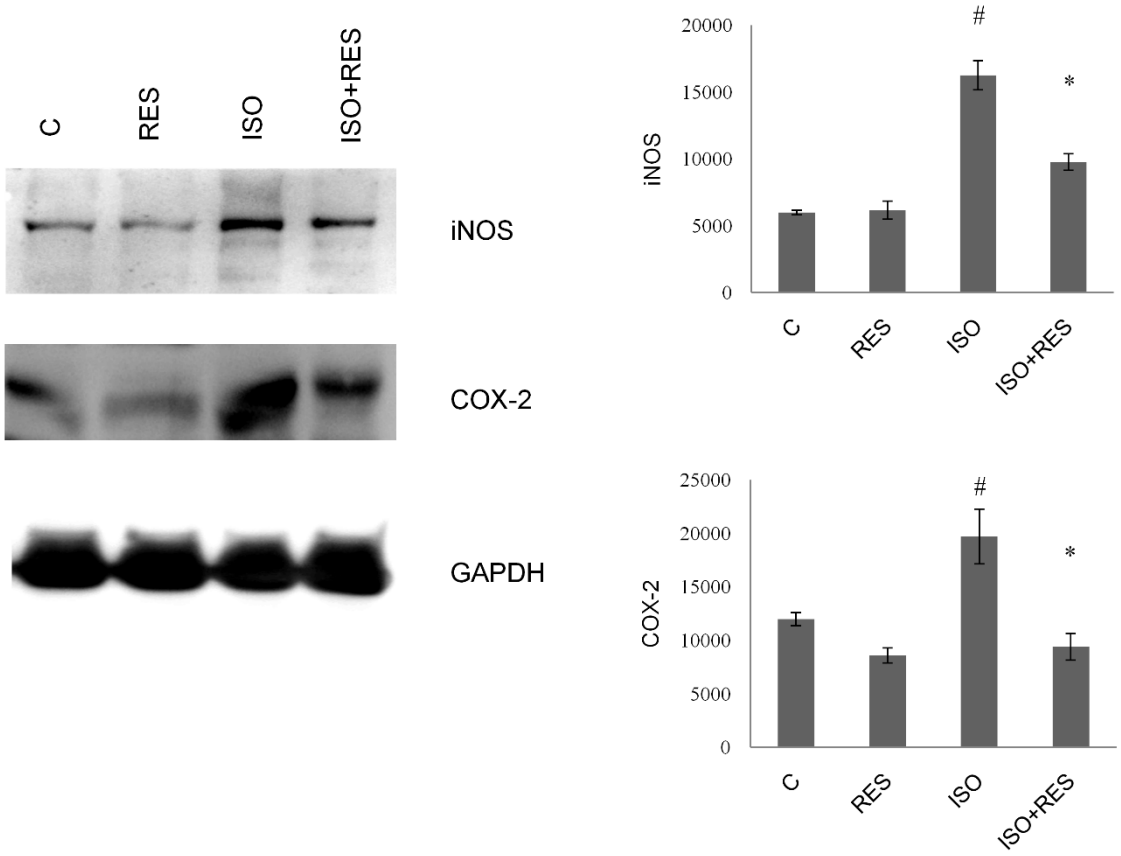

Fig 13. **Effect of resveratrol treatment on COX-2 and iNOS.** Representative western blot analysis of COX-2 and iNOS activation and densitometric evaluation is shown. GAPDH was used as a loading control. Representative blots and bar diagrams of three independent experiments are presented. C: control animals; RES: animals treated with resveratrol for 8 weeks; ISO: animals 8 weeks after ISO administration; ISO + RES: animals treated with resveratrol, 8 weeks after ISO administration. Values are mean ± SEM # $P<0.05$ Control vs. ISO, ∗$P<0.05$ ISO vs. ISO+RES.

5.3 Discussion

There are data in the literature about the protective effect of resveratrol on isoproterenol induced cardiac hypertrophy and on the earlier phase of remodeling (55, 83). Our working group has previously demonstrated the beneficial effects of an alcohol-free red wine extract in a postinfarction heart failure murine model (54). This time we aimed to test the cardioprotective effect of RES on oxidative stress and different signaling pathways in an advanced stage of heart failure. Subcutaneous administration of ISO produces patchy myocardial necrosis with subsequent hypertrophy, fibrosis and remodeling leading to heart failure similar to that observed in patients after myocardial infarction (65).

Plasma BNP levels, left ventricular wall thickness and dimensions were increased and the systolic left ventricular function was significantly decreased in ISO-treated animals. RES was capable of preserving LV function and moderated the severity of heart failure (Table 5.).

Excessive collagen deposition is the main histological characteristic of ventricular remodeling Damaged myocardium is replaced by scar tissue stabilizing the ventricular wall, but leading to systolic and diastolic dysfunction and arrhythmias. In our study RES prevented the marked fibrosis induced by ISO treatment (Fig 10A).

There is a large amount of evidence that ROS release plays a pivotal role in the development of heart failure (70). We observed increased immunohistochemical staining against nitrotyrosine (NT) -a marker of oxidative stress- on ISO-treated animal heart samples, which was significantly decreased by RES treatment (Fig 10B) indicating that RES was able to reduce myocardial ROS production. Excessive ROS formation induces different intracellular signaling pathways regulating cardiac remodeling, myocyte survival, apoptosis and necrosis (84).

In vitro studies have already shown that RES reduced the toxic effects of oxidative stress, decreased apoptosis via suppression of the p38-MAPK pathway, reduced autophagy and cell apoptosis through SIRT1 and the p-Akt pathway (58, 85-87). In animal studies, it was also proved that RES reversed LV remodeling and ameliorated heart failure after myocardial infarction by increasing the LC3-II/LC3-I ratio (60).

Here we investigated the effect of RES on the ERK 1/2, p38-MAPK, Akt-1 and GSK-3β pathways which play a critical role in cardiac hypertrophy and ventricular dilatation (88), myocyte survival, apoptosis, autophagy and necrosis (88-90). Akt activation inhibits cardiomyocyte apoptosis and improves surviving of cardiomyocytes in the ischemic heart (91). Akt exerts its protective effect through phosphorylation of the Bcl-2 family and GSK-3β (92). Akt-1 is a key molecule in the signaling of physiological hypertrophy and it has a pivotal role

in the prevention of pathological cardiac growth (88). In our investigation phosphorylation of Akt-1 and GSK-3β were elevated in all groups compared to the control group but the highest level of phosphorylations were in the ISO+RES group (Fig 11.), indicating that RES facilitated the activity of endogenous prosurvival signaling pathways.

There are conflicting data in the literature regarding the role of MAP kinases in the regulation of cell survival (27, 88, 89, 93-95). A wide variety of extra and intracellular stress signals can induce sequential phosphorylation and activation of MAPK kinases via phosphorylation on both threonine and tyrosine residues (90). Activation of MAPKs are observed in various heart diseases in humans and in the animal model of HCM, DCM, I/R injury and postinfarction heart failure (96, 97). It was shown that resveratrol can influence the activation of MAPK cascades (54, 96). In our study, the phosphorylation of p38-MAPK$^{\text{Thr180-Gly-Tyr182}}$ and ERK1/2$^{\text{Thr183-Tyr185}}$ was elevated in ISO-treated groups but RES treatment significantly decreased this elevation. These changes in the activation state of signaling molecules were probably due to the increased production of MAPK phospatase-1 (MKP-1) which is the major regulator of MAPKs (90, 95, 98). In accordance with this, the amount of MKP-1 was increased in the RES-treated groups compared to untreated animals (84, 86, 99).

Whereas COX-1 plays a housekeeping role, COX-2 plays a major part in inflammation, atherosclerosis and tumor formation (100-103). Previous studies showed that COX-2 is upregulated by p38-MAPK and ERK1/2 (24). Moreover, prolonged activation of COX-2 produces cardiac cell death, leading to gradual loss of myocardial function and eventually heart failure. We found in our postinfarction animal model that RES was able to reduce the activation of COX-2 induced by ISO treatment (Fig 13.).

Previous in vivo animal and human studies demonstrated the elevated expression of iNOS in heart failure (26). Overexpression of iNOS in the myocardium of mice resulted in peroxynitrite generation (104-107), and it has also been demonstrated that elevated nitrotyrosine formation results in an increase in iNOS levels, creating a vicious circle of harmful effects (108). These data indicates that iNOS is also a signifant factor in the development of postinfarction heart failure (109). In our study ISO increased both nitrotyrosin formation (Fig.10B) and iNOS activity (Fig.13.) which was efficiently attenuated by RES treatment. It has also been shown that iNOS, as well as COX-2 expression level is strongly correlated with the phosphorylation level of the MAPK-s (p38-MAPK and ERK1/2$^{\text{Thr183-Tyr185}}$) (110-112) suggesting a strong relation between oxidative stress and intracellular signal transduction.

In our study RES treatment moderated the severity of HF by decreasing oxidative stress, increasing the activity of pro-survival signaling pathways (Akt1, GSK-3β) and decreasing p38MAPK and ERK1/2 stress signaling pathways (Fig. 14.):

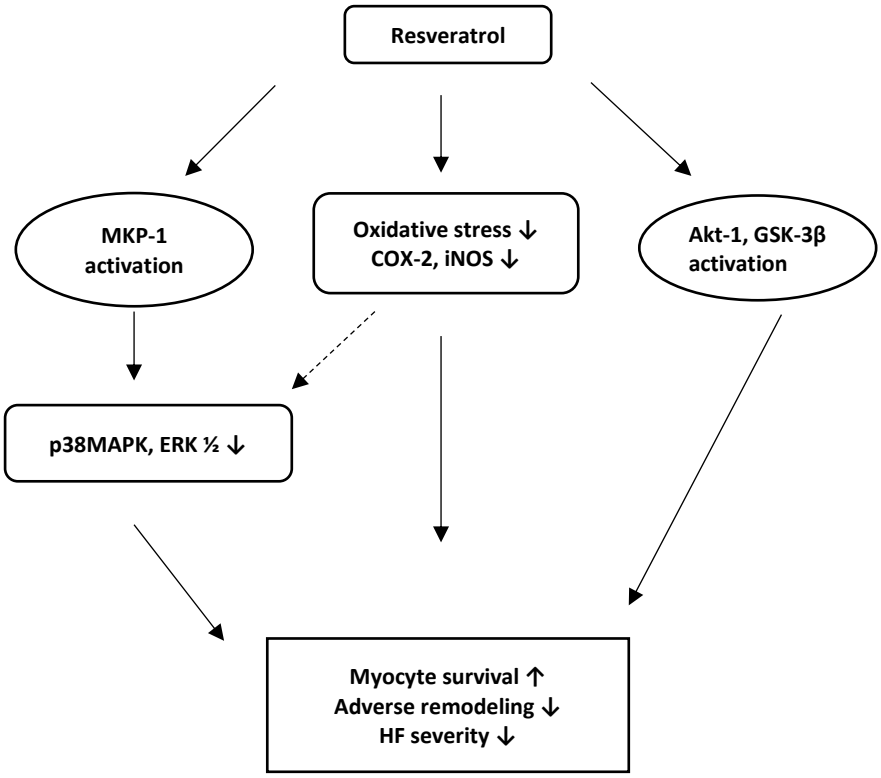

Fig 14. Summary of the beneficial effect of RES treatment in our HF model. Akt-1: RAC-alpha serine/threonine-protein kinase, COX: cyclooxygenase, ERK 1/2: extracellular signal-regulated kinase 1/2, GSK-3β: glycogen synthase kinase-3β, MAPK: mitogen-activated protein kinase, MKP-1: mitogen-activated protein (MAP) kinase-phophatase-1, iNOS: inducible nitric oxide synthase.

6 Summary of new findings

6.1 Summary of new findings of DOX treatment.

1. Our working group verified for the first time that DOX strikingly reduces the severity of postinfarction heart failure in an advanced stage of HF.

2. DOX protected mitochondria against ROS–induced mitochondrial fragmentation and prevented ROS–induced collapse of the mitochondrial membrane potential in H9c2 cardiomyocytes

3. DOX increased OPA-1 and decreased Mfn-2 level, and decreased the phosphorylation of Drp-1 in an ISO induced animal model of HF. Through these processes beneficially influenced mitochondrial dynamics and cell survival.

4. Presumably these new findings are mainly based upon its antioxidant property.

6.2 Summary of new findings of RES treatment in an ISO induced animal model of HF

1. RES improved left ventricular function, and decreased the VW/TL ratio, collagen deposition in the myocardium and the plasma BNP level.

2. RES exerted its beneficial effects through modifying several intracellular signaling pathways (Akt-1, GSK-3β, p38-MAPK, ERK1/2, MKP-1, COX-2 and iNOS).

3. The major effect of RES presumably based on its antioxidant capacity.

Both DOX and RES seems to be a promising agent in the future treatment of heart failure. Based on our findings they exerts these new cardioprotective effects mainly by decreasing the oxidative injury of the heart.

7 Acknowledgements

These studies were carried out at the Department of Biochemistry and Medical Chemistry and the 1st Department of Medicine, Medical School of the University of Pecs between 2013 and 2016.

I would like to express my thanks to my program leader, Professor Kálmán Tóth who gave a support and useful advises during my work, and to my project leaders Dr. Eszter Szabados and Dr. Róbert Halmosi who managed my experiments and helped me to perform echocardiographic examinations.

I am grateful to Professor Balázs Sümegi who taught me a biochemical way of thinking. He directed my work on the field of PARP inhibitors and he ensured the possibility of undisturbed work in his department for me.

I would like to express my gratitude to Professor Ferenc Gallyas, who gave me useful advices and help during the experiments.

Krisztián Erős, Dr. László Deres gave also a hand with a part of the experiments.

I am grateful to Istvánné Pásztor, Heléna Halasz, Bertalan Horváth and László Girán, who gave much assistance in the laboratory work.

I express my thanks to my family and friends for their encouraging support during my studies and work.

8 References

1. Ponikowski P, Voors AA, Anker SD, Bueno H, Cleland JG, Coats AJ, et al. 2016 ESC Guidelines for the diagnosis and treatment of acute and chronic heart failure: The Task Force for the diagnosis and treatment of acute and chronic heart failure of the European Society of Cardiology (ESC). Developed with the special contribution of the Heart Failure Association (HFA) of the ESC. Eur J Heart Fail. 2016;18(8):891-975.
2. Douglas Mann DZ, Peter Libby, Robert Bonow. Braunwald's Heart Disease: A Textbook of Cardiovascular Medicine, Single Volume. 10th ed2014. 2040 p.
3. Tschope C, Van Linthout S, Kherad B. Heart Failure with Preserved Ejection Fraction and Future Pharmacological Strategies: a Glance in the Crystal Ball. Curr Cardiol Rep. 2017;19(8):70.
4. Mosterd A, Hoes AW. Clinical epidemiology of heart failure. Heart. 932007. p. 1137-46.
5. Bui AL, Horwich TB, Fonarow GC. Epidemiology and risk profile of heart failure. Nat Rev Cardiol. 2011;8(1):30-41.
6. Jiang DS, Bian ZY, Zhang Y, Zhang SM, Liu Y, Zhang R, et al. Role of interferon regulatory factor 4 in the regulation of pathological cardiac hypertrophy. Hypertension. 2013;61(6):1193-202.
7. Sugamura K, Keaney JF, Jr. Reactive oxygen species in cardiovascular disease. Free Radic Biol Med. 2011;51(5):978-92.
8. Fillmore N, Lopaschuk GD. Targeting mitochondrial oxidative metabolism as an approach to treat heart failure. Biochim Biophys Acta. 2013;1833(4):857-65.
9. Halestrap AP, Pasdois P. The role of the mitochondrial permeability transition pore in heart disease. Biochim Biophys Acta. 2009;1787(11):1402-15.
10. Hafstad AD, Nabeebaccus AA, Shah AM. Novel aspects of ROS signalling in heart failure. Basic Res Cardiol. 2013;108(4):359.
11. Sawyer DB, Colucci WS. Mitochondrial Oxidative Stress in Heart Failure. 2000.
12. Ong SB, Subrayan S, Lim SY, Yellon DM, Davidson SM, Hausenloy DJ. Inhibiting mitochondrial fission protects the heart against ischemia/reperfusion injury. Circulation. 2010;121(18):2012-22.
13. Marin-Garcia J, Akhmedov AT, Moe GW. Mitochondria in heart failure: the emerging role of mitochondrial dynamics. Heart Fail Rev. 2013;18(4):439-56.

14. Wai T, Garcia-Prieto J, Baker MJ, Merkwirth C, Benit P, Rustin P, et al. Imbalanced OPA1 processing and mitochondrial fragmentation cause heart failure in mice. Science. 2015;350(6265):aad0116.

15. Alaimo A, Gorojod RM, Beauquis J, Munoz MJ, Saravia F, Kotler ML. Deregulation of mitochondria-shaping proteins Opa-1 and Drp-1 in manganese-induced apoptosis. PLoS One. 2014;9(3):e91848.

16. Shen T, Zheng M, Cao C, Chen C, Tang J, Zhang W, et al. Mitofusin-2 is a major determinant of oxidative stress-mediated heart muscle cell apoptosis. J Biol Chem. 2007;282(32):23354-61.

17. Brito OMd, Scorrano L. Mitofusin 2 tethers endoplasmic reticulum to mitochondria. Nature. 2008;456(7222):605-10.

18. Walter L, Hajnoczky G. Mitochondria and endoplasmic reticulum: the lethal interorganelle cross-talk. J Bioenerg Biomembr. 2005;37(3):191-206.

19. Papanicolaou KN, Khairallah RJ, Ngoh GA, Chikando A, Luptak I, O'Shea KM, et al. Mitofusin-2 Maintains Mitochondrial Structure and Contributes to Stress-Induced Permeability Transition in Cardiac Myocytes ▿†. Mol Cell Biol. 312011. p. 1309-28.

20. Knowlton AA, Chen L, Malik ZA. Heart Failure and Mitochondrial Dysfunction: The Role of Mitochondrial Fission/Fusion Abnormalities and New Therapeutic Strategies. J Cardiovasc Pharmacol. 2014;63(3):196-206.

21. Martens S, McMahon HT. Mechanisms of membrane fusion: disparate players and common principles. Nat Rev Mol Cell Biol. 2008;9(7):543-56.

22. Chen YR, Zweier JL. Cardiac mitochondria and reactive oxygen species generation. Circ Res. 2014;114(3):524-37.

23. Bartha E, Kiss GN, Kalman E, Kulcsár G, Kálai T, Hideg K, et al. Effect of L-2286, a poly(ADP-ribose)polymerase inhibitor and enalapril on myocardial remodeling and heart failure. J Cardiovasc Pharmacol. 2008;52(3):253-61.

24. Bujold K, Rhainds D, Jossart C, Febbraio M, Marleau S, Ong H. CD36-mediated cholesterol efflux is associated with PPARgamma activation via a MAPK-dependent COX-2 pathway in macrophages. Cardiovasc Res. 2009;83(3):457-64.

25. Boyd JH, Mathur S, Wang Y, Bateman RM, Walley KR. Toll-like receptor stimulation in cardiomyoctes decreases contractility and initiates an NF-κB dependent inflammatory response. 2006.

26. Vejlstrup NG, Bouloumie A, Boesgaard S, Andersen CB, Nielsen-Kudsk JE, Mortensen SA, et al. Inducible nitric oxide synthase (iNOS) in the human heart: expression and localization in congestive heart failure. J Mol Cell Cardiol. 1998;30(6):1215-23.

27. Palfi A, Toth A, Kulcsar G, Hanto K, Deres P, Bartha E, et al. The role of Akt and mitogen-activated protein kinase systems in the protective effect of poly(ADP-ribose) polymerase inhibition in Langendorff perfused and in isoproterenol-damaged rat hearts. J Pharmacol Exp Ther. 2005;315(1):273-82.

28. Grimm D, Elsner D, Schunkert H, Pfeifer M, Griese D, Bruckschlegel G, et al. Development of heart failure following isoproterenol administration in the rat: role of the renin-angiotensin system. Cardiovasc Res. 1998;37(1):91-100.

29. Deres L, Bartha E, Palfi A, Eros K, Riba A, Lantos J, et al. PARP-inhibitor treatment prevents hypertension induced cardiac remodeling by favorable modulation of heat shock proteins, Akt-1/GSK-3β and several PKC isoforms. PLoS One. 2014;9(7):e102148.

30. Yancy CW, Jessup M, Bozkurt B, Butler J, Casey DE, Jr., Drazner MH, et al. 2013 ACCF/AHA guideline for the management of heart failure: a report of the American College of Cardiology Foundation/American Heart Association Task Force on Practice Guidelines. J Am Coll Cardiol. 2013;62(16):e147-239.

31. Yancy CW, Jessup M, Bozkurt B, Butler J, Casey DE, Jr., Colvin MM, et al. 2017 ACC/AHA/HFSA Focused Update of the 2013 ACCF/AHA Guideline for the Management of Heart Failure: A Report of the American College of Cardiology/American Heart Association Task Force on Clinical Practice Guidelines and the Heart Failure Society of America. J Card Fail. 2017.

32. Tarone G, Balligand JL, Bauersachs J, Clerk A, De Windt L, Heymans S, et al. Targeting myocardial remodelling to develop novel therapies for heart failure: a position paper from the Working Group on Myocardial Function of the European Society of Cardiology. Eur J Heart Fail. 2014;16(5):494-508.

33. Bartha E, Solti I, Kereskai L, Lantos J, Plozer E, Magyar K, et al. PARP inhibition delays transition of hypertensive cardiopathy to heart failure in spontaneously hypertensive rats. Cardiovasc Res. 2009;83(3):501-10.

34. Godefroy E, Gallois A, Idoyaga J, Merad M, Tung N, Monu N, et al. Activation of toll-like receptor-2 by endogenous matrix metalloproteinase-2 modulates dendritic-cell-mediated inflammatory responses. Cell Rep. 2014;9(5):1856-70.

35. Hughes BG, Schulz R. Targeting MMP-2 to treat ischemic heart injury. Basic Res Cardiol. 2014;109(4):424.

36. Errami M, Galindo CL, Tassa AT, Dimaio JM, Hill JA, Garner HR. Doxycycline attenuates isoproterenol- and transverse aortic banding-induced cardiac hypertrophy in mice. J Pharmacol Exp Ther. 2008;324(3):1196-203.

37. Hori Y, Kunihiro S, Sato S, Yoshioka K, Hara Y, Kanai K, et al. Doxycycline attenuates isoproterenol-induced myocardial fibrosis and matrix metalloproteinase activity in rats. Biol Pharm Bull. 2009;32(10):1678-82.

38. Schulze CJ, Castro MM, Kandasamy AD, Cena J, Bryden C, Wang SH, et al. Doxycycline reduces cardiac matrix metalloproteinase-2 activity but does not ameliorate myocardial dysfunction during reperfusion in coronary artery bypass patients undergoing cardiopulmonary bypass. Crit Care Med. 2013;41(11):2512-20.

39. Spinale FG. Matrix metalloproteinases: regulation and dysregulation in the failing heart. Circ Res. 2002;90(5):520-30.

40. Golub LM, Ciancio S, Ramamamurthy NS, Leung M, McNamara TF. Low-dose doxycycline therapy: effect on gingival and crevicular fluid collagenase activity in humans. J Periodontal Res. 1990;25(6):321-30.

41. Modrak JB, Rovang KS. Estimation of infarct size by determination of myocardial 3H-tetracycline accumulation in the coronary ligated rat. Res Commun Chem Pathol Pharmacol. 1981;34(1):149-52.

42. Griffin MO, Fricovsky E, Ceballos G, Villarreal F. Tetracyclines: a pleitropic family of compounds with promising therapeutic properties. Review of the literature. Am J Physiol Cell Physiol. 2010;299(3):C539-48.

43. Ducharme A, Frantz S, Aikawa M, Rabkin E, Lindsey M, Rohde LE, et al. Targeted deletion of matrix metalloproteinase-9 attenuates left ventricular enlargement and collagen accumulation after experimental myocardial infarction. J Clin Invest. 2000;106(1):55-62.

44. Webb CS, Bonnema DD, Ahmed SH, Leonardi AH, McClure CD, Clark LL, et al. Specific temporal profile of matrix metalloproteinase release occurs in patients after myocardial infarction: relation to left ventricular remodeling. Circulation. 2006;114(10):1020-7.

45. Garcia RA, Go KV, Villarreal FJ. Effects of timed administration of doxycycline or methylprednisolone on post-myocardial infarction inflammation and left ventricular remodeling in the rat heart. Mol Cell Biochem. 2007;300(1-2):159-69.

46. Wang W, Schulze CJ, Suarez-Pinzon WL, Dyck JR, Sawicki G, Schulz R. Intracellular action of matrix metalloproteinase-2 accounts for acute myocardial ischemia and reperfusion injury. Circulation. 2002;106(12):1543-9.

47. Cheung PY, Sawicki G, Wozniak M, Wang W, Radomski MW, Schulz R. Matrix metalloproteinase-2 contributes to ischemia-reperfusion injury in the heart. Circulation. 2000;101(15):1833-9.

48. Cerisano G, Buonamici P, Valenti R, Sciagra R, Raspanti S, Santini A, et al. Early short-term doxycycline therapy in patients with acute myocardial infarction and left ventricular dysfunction to prevent the ominous progression to adverse remodelling: the TIPTOP trial. Eur Heart J. 2014;35(3):184-91.

49. Dolinsky VW, Rogan KJ, Sung MM, Zordoky BN, Haykowsky MJ, Young ME, et al. Both aerobic exercise and resveratrol supplementation attenuate doxorubicin-induced cardiac injury in mice. Am J Physiol Endocrinol Metab. 2013;305(2):E243-53.

50. Tome-Carneiro J, Larrosa M, Gonzalez-Sarrias A, Tomas-Barberan FA, Garcia-Conesa MT, Espin JC. Resveratrol and clinical trials: the crossroad from in vitro studies to human evidence. Curr Pharm Des. 2013;19(34):6064-93.

51. Raj P, Louis XL, Thandapilly SJ, Movahed A, Zieroth S, Netticadan T. Potential of resveratrol in the treatment of heart failure. Life Sci. 2014;95(2):63-71.

52. Burstein B, Maguy A, Clement R, Gosselin H, Poulin F, Ethier N, et al. Effects of resveratrol (trans-3,5,4'-trihydroxystilbene) treatment on cardiac remodeling following myocardial infarction. J Pharmacol Exp Ther. 2007;323(3):916-23.

53. Yoshida Y, Shioi T, Izumi T. Resveratrol ameliorates experimental autoimmune myocarditis. Circ J. 2007;71(3):397-404.

54. Palfi A, Bartha E, Copf L, Mark L, Gallyas F, Veres B, et al. Alcohol-free red wine inhibits isoproterenol-induced cardiac remodeling in rats by the regulation of Akt1 and protein kinase C alpha/beta II. J Nutr Biochem. 2009;20(6):418-25.

55. Sung MM, Dyck JR. Therapeutic potential of resveratrol in heart failure. Ann N Y Acad Sci. 2015;1348(1):32-45.

56. Csiszar A. Anti-inflammatory effects of resveratrol: possible role in prevention of age-related cardiovascular disease. Ann N Y Acad Sci. 2011;1215:117-22.

57. Das S, Das DK. Anti-inflammatory responses of resveratrol. Inflamm Allergy Drug Targets. 2007;6(3):168-73.

58. Hashemzaei M, Entezari Heravi R, Rezaee R, Roohbakhsh A, Karimi G. Regulation of autophagy by some natural products as a potential therapeutic strategy for cardiovascular disorders. Eur J Pharmacol. 2017;802:44-51.

59. Gu XS, Wang ZB, Ye Z, Lei JP, Li L, Su DF, et al. Resveratrol, an activator of SIRT1, upregulates AMPK and improves cardiac function in heart failure. Genet Mol Res. 2014;13(1):323-35.
60. Kanamori H, Takemura G, Goto K, Tsujimoto A, Ogino A, Takeyama T, et al. Resveratrol reverses remodeling in hearts with large, old myocardial infarctions through enhanced autophagy-activating AMP kinase pathway. Am J Pathol. 2013;182(3):701-13.
61. Magyar K, Halmosi R, Palfi A, Feher G, Czopf L, Fulop A, et al. Cardioprotection by resveratrol: A human clinical trial in patients with stable coronary artery disease. Clin Hemorheol Microcirc. 2012;50(3):179-87.
62. Papazisis KT, Geromichalos GD, Dimitriadis KA, Kortsaris AH. Optimization of the sulforhodamine B colorimetric assay. J Immunol Methods. 1997;208(2):151-8.
63. Palfi A, Toth A, Hanto K, Deres P, Szabados E, Szereday Z, et al. PARP inhibition prevents postinfarction myocardial remodeling and heart failure via the protein kinase C/glycogen synthase kinase-3beta pathway. J Mol Cell Cardiol. 2006;41(1):149-59.
64. Liaudet L, Soriano FG, Szabó É, Virág L, Mabley JG, Salzman AL, et al. Protection against hemorrhagic shock in mice genetically deficient in poly(ADP-ribose)polymerase. 2000.
65. Teerlink JR, Pfeffer JM, Pfeffer MA. Progressive ventricular remodeling in response to diffuse isoproterenol-induced myocardial necrosis in rats. Circ Res. 1994;75(1):105-13.
66. Roberts AW, Clark AL, Witte KK. Review article: Left ventricular dysfunction and heart failure in metabolic syndrome and diabetes without overt coronary artery disease--do we need to screen our patients? Diab Vasc Dis Res. 2009;6(3):153-63.
67. Chung AWY, Yang HHC, Radomski MW, Breemen Cv. Long-Term Doxycycline Is More Effective Than Atenolol to Prevent Thoracic Aortic Aneurysm in Marfan Syndrome Through the Inhibition of Matrix Metalloproteinase-2 and -9. 2008.
68. Camp TM, Tyagi SC, Aru GM, Hayden MR, Mehta JL. Doxycycline ameliorates ischemic and border-zone remodeling and endothelial dysfunction after myocardial infarction in rats. J Heart Lung Transplant. 2004;23(6):729-36.
69. Grieve DJ, Shah AM. Oxidative stress in heart failure. 2003.
70. Okonko DO, Shah AM. Heart failure: Mitochondrial dysfunction and oxidative stress in CHF. Nature Reviews Cardiology. 2014;12:6-8.
71. Ozcinar E, Okatan EN, Tuncay E, Eryilmaz S, Turan B. Improvement of functional recovery of donor heart following cold static storage with doxycycline cardioplegia. Cardiovasc Toxicol. 2014;14(1):64-73.

72. Elewa MA, Al-Gayyar MM, Schaalan MF, Abd El Galil KH, Ebrahim MA, El-Shishtawy MM. Hepatoprotective and anti-tumor effects of targeting MMP-9 in hepatocellular carcinoma and its relation to vascular invasion markers. Clin Exp Metastasis. 2015;32(5):479-93.

73. Antonio RC, Ceron CS, Rizzi E, Coelho EB, Tanus-Santos JE, Gerlach RF. Antioxidant effect of doxycycline decreases MMP activity and blood pressure in SHR. Mol Cell Biochem. 2014;386(1-2):99-105.

74. Gupte TM. Mitochondrial Fragmentation Due to Inhibition of Fusion Increases Cyclin B through Mitochondrial Superoxide Radicals. PLoS One. 2015;10(5):e0126829.

75. Giacomotto J, Brouilly N, Walter L, Mariol MC, Berger J, Segalat L, et al. Chemical genetics unveils a key role of mitochondrial dynamics, cytochrome c release and IP3R activity in muscular dystrophy. Hum Mol Genet. 2013;22(22):4562-78.

76. Harijith A, Ebenezer DL, Natarajan V. Reactive oxygen species at the crossroads of inflammasome and inflammation. Front Physiol. 2014;5:352.

77. Di Lisa F, Bernardi P. Mitochondria and ischemia-reperfusion injury of the heart: fixing a hole. Cardiovasc Res. 2006;70(2):191-9.

78. Sharov VG, Todor AV, Imai M, Sabbah HN. Inhibition of mitochondrial permeability transition pores by cyclosporine A improves cytochrome C oxidase function and increases rate of ATP synthesis in failing cardiomyocytes. Heart Fail Rev. 2005;10(4):305-10.

79. Walter L, Miyoshi H, Leverve X, Bernard P, Fontaine E. Regulation of the mitochondrial permeability transition pore by ubiquinone analogs. A progress report. Free Radic Res. 2002;36(4):405-12.

80. Novgorodov SA, Gudz TI, Obeid LM. Long-chain Ceramide Is a Potent Inhibitor of the Mitochondrial Permeability Transition Pore*. J Biol Chem. 2832008. p. 24707-17.

81. Mukherjee S, Dudley JI, Das DK. Dose-Dependency of Resveratrol in Providing Health Benefits. Dose Response. 82010. p. 478-500.

82. Juan ME, Vinardell MP, Planas JM. The daily oral administration of high doses of trans-resveratrol to rats for 28 days is not harmful. J Nutr. 2002;132(2):257-60.

83. Chakraborty S, Pujani M, Haque SE. Combinational effect of resveratrol and atorvastatin on isoproterenol-induced cardiac hypertrophy in rats. J Pharm Bioallied Sci. 72015. p. 233-8.

84. Park ES, Kang DH, Kang JC, Jang YC, Lee MJ, Chung HJ, et al. Cardioprotective effect of KR-33889, a novel PARP inhibitor, against oxidative stress-induced apoptosis in H9c2 cells and isolated rat hearts. Arch Pharm Res. 2017.

85. Huang H, Chen G, Liao D, Zhu Y, Pu R, Xue X. The effects of resveratrol intervention on risk markers of cardiovascular health in overweight and obese subjects: a pooled analysis of randomized controlled trials. Obes Rev. 2016;17(12):1329-40.

86. Zhou M, Wang S, Zhao A, Wang K, Fan Z, Yang H, et al. Transcriptomic and metabonomic profiling reveal synergistic effects of quercetin and resveratrol supplementation in high fat diet fed mice. J Proteome Res. 2012;11(10):4961-71.

87. Dutta D, Xu J, Dirain ML, Leeuwenburgh C. Calorie restriction combined with resveratrol induces autophagy and protects 26-month-old rat hearts from doxorubicin-induced toxicity. Free Radic Biol Med. 2014;74:252-62.

88. Heineke J, Molkentin JD. Regulation of cardiac hypertrophy by intracellular signalling pathways. Nature Reviews Molecular Cell Biology. 2006;7(8):589-600.

89. Bognar E, Sarszegi Z, Szabo A, Debreceni B, Kalman N, Tucsek Z, et al. Antioxidant and anti-inflammatory effects in RAW264.7 macrophages of malvidin, a major red wine polyphenol. PLoS One. 2013;8(6):e65355.

90. Kondoh K, Nishida E. Regulation of MAP kinases by MAP kinase phosphatases. Biochim Biophys Acta. 2007;1773(8):1227-37.

91. Matsui T, Tao J, del Monte F, Lee KH, Li L, Picard M, et al. Akt activation preserves cardiac function and prevents injury after transient cardiac ischemia in vivo. Circulation. 2001;104(3):330-5.

92. Miyamoto S, Murphy AN, Brown JH. Akt mediated mitochondrial protection in the heart: metabolic and survival pathways to the rescue. J Bioenerg Biomembr. 2009;41(2):169-80.

93. Xia Z, Dickens M, Raingeaud J, Davis RJ, Greenberg ME. Opposing effects of ERK and JNK-p38 MAP kinases on apoptosis. Science. 1995;270(5240):1326-31.

94. Veres B, Radnai B, Gallyas F, Varbiro G, Berente Z, Osz E, et al. Regulation of Kinase Cascades and Transcription Factors by a Poly(ADP-Ribose) Polymerase-1 Inhibitor, 4-Hydroxyquinazoline, in Lipopolysaccharide-Induced Inflammation in Mice. 2004.

95. Racz B, Hanto K, Tapodi A, Solti I, Kalman N, Jakus P, et al. Regulation of MKP-1 expression and MAPK activation by PARP-1 in oxidative stress: a new mechanism for the cytoplasmic effect of PARP-1 activation. Free Radic Biol Med. 2010;49(12):1978-88.

96. El-Mowafy AM, White RE. Resveratrol inhibits MAPK activity and nuclear translocation in coronary artery smooth muscle: reversal of endothelin-1 stimulatory effects. FEBS Lett. 1999;451(1):63-7.

97. Gao Y, Kang L, Li C, Wang X, Sun C, Li Q, et al. Resveratrol Ameliorates Diabetes-Induced Cardiac Dysfunction Through AT1R-ERK/p38 MAPK Signaling Pathway. Cardiovasc Toxicol. 2016;16(2):130-7.

98. Andrews CS, Matsuyama S, Lee BC, Li JD. Resveratrol suppresses NTHi-induced inflammation via up-regulation of the negative regulator MyD88 short. Sci Rep. 2016;6:34445.

99. Kim GS, Choi YK, Song SS, Kim WK, Han BH. MKP-1 contributes to oxidative stress-induced apoptosis via inactivation of ERK1/2 in SH-SY5Y cells. Biochem Biophys Res Commun. 2005;338(4):1732-8.

100. Cipollone F, Fazia ML. COX-2 and atherosclerosis. J Cardiovasc Pharmacol. 2006;47 Suppl 1:S26-36.

101. Linton MF, Fazio S. Cyclooxygenase-2 and inflammation in atherosclerosis. Curr Opin Pharmacol. 2004;4(2):116-23.

102. Burleigh ME, Babaev VR, Yancey PG, Major AS, McCaleb JL, Oates JA, et al. Cyclooxygenase-2 promotes early atherosclerotic lesion formation in ApoE-deficient and C57BL/6 mice. J Mol Cell Cardiol. 2005;39(3):443-52.

103. O'Leary KA, de Pascual-Teresa S, Needs PW, Bao YP, O'Brien NM, Williamson G. Effect of flavonoids and vitamin E on cyclooxygenase-2 (COX-2) transcription. Mutat Res. 2004;551(1-2):245-54.

104. Starling RC. Inducible nitric oxide synthase in severe human heart failure: impact of mechanical unloading. J Am Coll Cardiol. 45. United States2005. p. 1425-7.

105. Xia Y, Zweier JL. Superoxide and peroxynitrite generation from inducible nitric oxide synthase in macrophages. Proc Natl Acad Sci U S A. 1997;94(13):6954-8.

106. Kumar A, Chen SH, Kadiiska MB, Hong JS, Zielonka J, Kalyanaraman B, et al. Inducible nitric oxide synthase is key to peroxynitrite-mediated, LPS-induced protein radical formation in murine microglial BV2 cells. Free Radic Biol Med. 2014;73:51-9.

107. Cotton JM, Kearney MT, Shah AM. Nitric oxide and myocardial function in heart failure: friend or foe? Heart. 882002. p. 564-6.

108. Cooke CL, Davidge ST. Peroxynitrite increases iNOS through NF-kappaB and decreases prostacyclin synthase in endothelial cells. Am J Physiol Cell Physiol. 2002;282(2):C395-402.

109. Lamon BD, Upmacis RK, Deeb RS, Koyuncu H, Hajjar DP. Inducible nitric oxide synthase gene deletion exaggerates MAPK-mediated cyclooxygenase-2 induction by inflammatory stimuli. Am J Physiol Heart Circ Physiol. 2010;299(3):H613-23.

110. Xia Q, Hu Q, Wang H, Yang H, Gao F, Ren H, et al. Induction of COX-2-PGE2 synthesis by activation of the MAPK|[sol]|ERK pathway contributes to neuronal death triggered by TDP-43-depleted microglia. Cell Death & Disease. 2015;6(3).
111. Chae HS, Kang OH, Lee YS, Choi JG, Oh YC, Jang HJ, et al. Inhibition of LPS-induced iNOS, COX-2 and inflammatory mediator expression by paeonol through the MAPKs inactivation in RAW 264.7 cells. Am J Chin Med. 2009;37(1):181-94.
112. Liou CJ, Len WB, Wu SJ, Lin CF, Wu XL, Huang WC. Casticin inhibits COX-2 and iNOS expression via suppression of NF-kappaB and MAPK signaling in lipopolysaccharide-stimulated mouse macrophages. J Ethnopharmacol. 2014;158 Pt A:310-6.

9 Publications of the author

Papers

ADAM RIBA LASZLO DERES, KRISZTIAN EROS, ALIZ SZABO, KLARA MAGYAR, BALAZS SUMEGI, KALMAN TOTH, ROBERT HALMOSI, ESZTER SZABADOS. (2017) Doxycycline protects against ROS-induced mitochondrial fragmentation and ISO-induced heart failure. PLoS ONE 12(4): e0175195. doi:10.1371/journal.pone.0175195

KRISZTIAN EROS, KLARA MAGYAR, LASZLO DERES, ARPAD SKAZEL, ADAM RIBA, ZOLTAN VAMOS, TAMAS KALAI, FERENC GALLYAS JR., BALAZS SUMEGI. (2017) Chronic PARP-1 inhibition reduces carotid vessel remodeling and oxidative damage of the dorsal hippocampus in spontaneously hypertensive rats. PLoS ONE 12(3): e0174401.
https://doi.org/10.1371/journal.pone.0174401

LASZLO DERES, EVA BARTHA, ANITA PALFI, KRISZTIAN EROS, ADAM RIBA, JANOS LANTOS, TAMAS KALAI, KALMAN HIDEG, BALAZS SUMEGI, FERENC GALLYAS, KALMAN TOTH, ROBERT HALMOSI
PARP-Inhibitor Treatment Prevents Hypertension Induced Cardiac Remodeling by Favorable Modulation of Heat Shock Proteins, Akt-1/GSK-3β and Several PKC Isoforms
PLoS One. 2014; 9(7): e102148. Published online 2014 July 11. doi: 10.1371/journal.pone.010214

Abstracts

MAGYAR K., RIBA Á.,VÁMOS Z., BALOGH A.,DERES L., HIDEG K., SÜMEGI B., KOLLER Á.,HALMOSI R., TÓTH K., Az Akt és a MAP kináz szerepe a krónikus hipertenzív patkány modellben

a PARP gátlás által kiváltott védelemben. A Magyar Kardiológusok Társasága 2011. évi Tudományos Kongresszusa, 2011. május 1-14., Balatonfüred.

MAGYAR K., RIBA Á., VÁMOS Z., BALOGH A., DERES L., HIDEG K., SÜMEGI B., KOLLER Á.,HALMOSI R., TÓTH K., The role of akt and mitogen-activated protein kinase systems int he protective effect of PARP inhibition in a chronic hypertensive rat model. FAMÉ 2011. június 8-11., Pécs

MAGYAR K., RIBA Á., VÁMOS Z., BALOGH A., DERES L., HIDEG K., SÜMEGI B., KOLLER Á.,HALMOSI R., TÓTH K., Az L-2286 jelű PARP-gátló vegyület lehetséges szerepe a mitokondriális őssejt regenerációban. A Magyar Kardiológusok Társasága 2012. évi Tudományos Kongresszusa, 2012. május 9-12., Balatonfüred.

MAGYAR, K, RIBA A., VAMOS, Z., BALOGH, A., DERES, L., HIDEG, K., SUMEGI, B., KOLLER, A., HALMOSI, R., TOTH, K. The role of Akt and mitogen-activated protein kinase systems in the vasoprotection elicited by PARP inhibition in hypertensive rats. Congress of the European Society of Cardiology, August 27-31, 2011, Paris, France, Eur. Heart J, 32 (Abstract Supplement), 34, 2011.

ERŐS K., DERES L., MAGYAR K., RIBA Á., HIDEG K., SERESS L., SÜMEGI B., TÓTH K., HALMOSI R. A PARP1-gátlás hatása a mitokondriumok fragmentációjára in vivo SHR modellben. A Magyar Kardiológusok Társasága 2013. évi Tudományos Kongresszusa, 2013. május 8–11., Balatonfüred, Card. Hung. Suppl. 2013; 43; B16.

RIBA Á., DERES L., ERŐS K., SÜMEGI B., TÓTH K., HALMOSI R., SZABADOS E.
A doxycycline hatása az isoproterenol indukálta szívelégtelenség kialakulásásra. A Magyar Kardiológusok Társasága 2013. évi Tudományos Kongresszusa, 2015. május 6-9., Balatonfüred, Card. Hung. Suppl. 2015

A. RIBA L. DERES, K. EROS, A. SZABO, B. SUMEGI, K. TOTH, R. HALMOSI, E. SZABADOS
Doxycycline protects against ROS-induced mitochondrial fragmentation and ISO-induced heart failure. European Society of Cardiology Heart Failure Congress, Firenze, 2016.

RIBA Á., DERES L., ERŐS K., SÜMEGI B., TÓTH K., , SZABADOS E, HALMOSI R.
A rezveratrol hatása a posztinfarktusos szívelégtelenség kialakulására állatmodellen. A Magyar Kardiológusok Társasága 2016. évi Tudományos Kongresszusa, 2016. május 5-7., Balatonfüred, Card. Hung. Suppl. 2016

RIBA Á., NAGYNÉ-KISS GY., DERES L., SÜMEGI B., TÓTH K., HALMOSI R
A poli(ADP-ribóz) polimeráz (PARP) gátló HO-3089 védő hatása iszkémia-reperfúzióban a megnövelt myocardiális glükóz-felvételen keresztül A Magyar Kardiológusok Társasága 2017. évi Tudományos Kongresszusa, 2017. május 10-13., Balatonfüred, Card. Hung. Suppl. 2017